T125
26

To the Graduate Council:

I am submitting herewith a thesis written by Voreata Anne Sanders Waddell entitled "Mie Analysis of Geometries for Phase Angle Particle Sizing Interferometry." I have examined the final copy of this thesis for form and content and recommend that it be accepted in partial fulfillment of the requirements for the degree of Master of Science, with a major in Physics.

Thomas V. Giel Jr.

Thomas V. Giel, Jr., Major Professor

We have read this thesis
and recommend its acceptance:

Roy J. Schulz

Arthur A. Mason

Accepted for the Council:

CW Minkel

Vice Provost
and Dean of The Graduate School

STATEMENT OF PERMISSION TO USE

In presenting this thesis in partial fulfillment of the requirements for a Master's degree at The University of Tennessee, Knoxville, I agree that the Library shall make it available to borrowers under rules of the Library. Brief quotations from this thesis are allowable without special permission, provided that accurate acknowledgment of source is made.

Permission of extensive quotation from or reproduction of this thesis may be granted by my major professor, or in his absence, by the Head of Interlibrary Services when, in the opinion of either, the proposed use of the material is for scholarly purposes. Any copying or use of the material in this thesis for financial gain shall not be allowed without my written permission.

Signature Vreata Anne Sanders Waddell

Date August 12, 1986

MIE ANALYSIS OF GEOMETRIES FOR PHASE ANGLE PARTICLE SIZING INTERFEROMETRY

A Thesis

Presented for the

Master of Science

Degree

The University of Tennessee, Knoxville

Voreata Anne Sanders Waddell

August 1986

DEDICATION

This thesis is dedicated to my husband, Dr. Thomas G. Waddell and my sons, David G. Perry, Christopher T. Perry, Sean P. Perry, Nicklaus A. Waddell and Samuel L. Waddell.

ACKNOWLEDGMENTS

The work reported herein was supported by The University of Tennessee Space Institute Energy Conversion Research and Development Programs under Contract Nos. DE-AC21-85MC22184 and DE-AC02-79ET10815.

The author would like to express her appreciation to the members of her committee, Dr. Thomas V. Giel, Jr., Chairman, Dr. Roy J. Schulz and Dr. Arthur A. Mason. Appreciation is also expressed to Dr. Jung Young Son for his assistance with the laser velocimeter, the Lorentz-Mie light scattering code and the PSI signal prediction codes used in the study. His considerable assistance with operating and interpreting results from these codes made this study possible. Further appreciation is expressed to Dr. James M. Henry, Dr. Stephanie Smullen, Mr. Mike Robinson, Mr. Don Elrod, Ms. Becky Bass, and the UTC Computer Center of Excellence for their assistance in implementing these codes on the IBM 4381 Level 2 and the many hours of CPU time provided. Finally, special appreciation is expressed to Ms. Madge Gibson for typing the thesis to comply with the exacting University stipulations.

The author gratefully acknowledges Dr. Jim Ware and Dr. John Trimpey of The University of Tennessee Chattanooga for granting her a leave of absence to pursue graduate study.

ABSTRACT

The phase of the Doppler signal component obtained with a laser Doppler velocimeter was examined analytically for particle sizing applications. The analysis used a complete Lorentz-Mie scattering code capable of predicting the light scattered by spheres, of arbitrary index of refraction, into any designated solid angle located at any designated position relative to the particle coordinates and the Poynting vectors of the multiple input beams. The purpose of this project is to provide extensive, full Mie predictions of the phase-size relation, using laser Doppler velocimeter phase measurements, particularly for the 0.3 to 6 μm size range. Phase information was compared to several other in-situ laser particle sizing interferometer measurements to identify its comparative advantages and disadvantages. Because phase is a function of optical geometry including fringe spacing, collector location, and collector focal length, and of particle index of refraction, as well as particle size, Mie scattering predictions were computed for numerous optical geometries and particle indices of refraction. The approach taken was to use the UTSI developed Mie Code, incorporating Pendleton's solution and Son's algorithms to provide extensive predictions of the variations of the LV signal characteristics. This allowed identification of promising optical setups for optimizing in-situ particle sizing for the 0.3 to 6.2 micron diameter range with index of refraction variations of 1.1 to 3.5.

TABLE OF CONTENTS

LIST OF FIGURES

FIGURE | PAGE

CHAPTER I

INTRODUCTION

Need for Particle Sizing

The scientific and engineering community has long been interested in the problem of particle sizing, counting and detection. Health scientists are interested in particulates because of environmental concerns. Their interests range from particulate pollution (e.g. soot emitted from diesels) to the introduction of sorbent particulates in SO_x and NO_x scrubbers. For example, soot formed during combustion processes has properties of interest to both researchers and designers involved in process and system development in the field of power generation, from magnetohydrodynamic power plants to gas turbine engines. Also, for scientists interested in obscurants for military defense applications, particle characterization is of critical concern.

Intrusive Methods

Because of the multidisciplinary interest in particle characterization, various schemes have been proposed to detect, count and size particles entrained by or suspended in fluid flow. In laminar flows samples can be extracted and analyzed to obtain desired particulate mass loading, and size distribution information. The advantages of performing measurements with extractive sampling are that an actual mass measurement can be made, physical and chemical properties can be analyzed, and extractive sampling results are accepted by industry and the Environmental Protection Agency. Disadvantages of extractive sampling are that it is an intrusive technique that disturbes the flow being sampled, and it is both tedious and time consuming, preventing the sample from being analyzed in real time, and the process is labor intensive. In addition, when sampling dust suspended in gas streams, it is difficult to obtain a representative sample unless the aspiration velocity of the probe equals the gas velocity of the probe tip. When this can be done, the sampling process is called isokinetic sampling. As shown in Figure 1, to sample isokinetically, the probe should not perturb the gas streamlines, so that only the particles in the projected area of the probe will enter the probe [1]. Anisokinetic sampling occurs when the sampling velocity differs from that of the gas stream. When the gas streamlines are disturbed by the probe extraction, either the number of particles per volume of entrained gas entering the probe can differ from those that would be in the mainstream, or the particle size distribution can be biased by centrifugal separation effects from that in the mainstream, or both. If the streamlines approaching the probe are unsteady, isokinetic sampling cannot be guaranteed. Therefore, since most industrial flows are turbulent, representative samples are difficult to extract. Of particular difficulty are turbulent flows of high temperature, and burning flows, where particle characterization is extremely important for combustion control and diagnosis. Further, even when a representative sample can be extracted, particulate agglomeration, fracturing and settling can occur within the sampling flow train, which will make the analyzed extractive samples non-representative. Thus, a non-intrusive, non-extractive in-situ method for particle cloud diagnosis

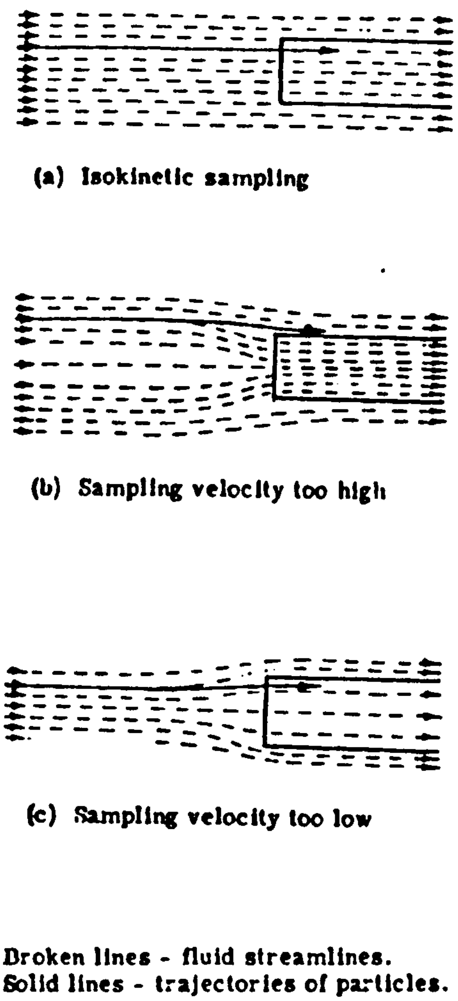

Figure 1. Fluid Flow Patterns and Possible Particle Paths Under Conditions of Isokinetic and Anisokinetic Sampling.

is desirable because the measurements should provide the true particulate size distribution, come from an undisturbed flow, and can be monitored continuously.

Non-intrusive Methods

The majority of non-intrusive, in-situ methods which have been proposed are based on measurements of light scattered by the particles in the flow. Laser holography and the Knollenberg probe are not considered in this discussion because they are not applicable to the size range of interest. Light-scattering methods are useful for particles with sizes the same order of magnitude as the incident radiation wavelengths. Self [2] described in-situ optical sizing in combustion systems, and pointed out that optical access considerations in combustion systems often restrict the range of particle number densities that can be measured at any one time. The principal techniques were categorized by Self [2] as ensemble methods and single particle counters. Ensemble methods are useful for large number densities, where there are many particles in the control volume at the same time. Ensemble scattering methods are also less susceptible to beam wander. Beam wander, which changes the effective optical system alignment, is due to fluctuating gas composition and temperature gradients. The severity of the beam wander effects depends on the type of instrument used and the nature and size of the combustion system, as shown in Figure 2. Generally, ensemble methods provide some measure of mean size and/or particle number densities, and with some optical arrangements, a most probable size distribution.

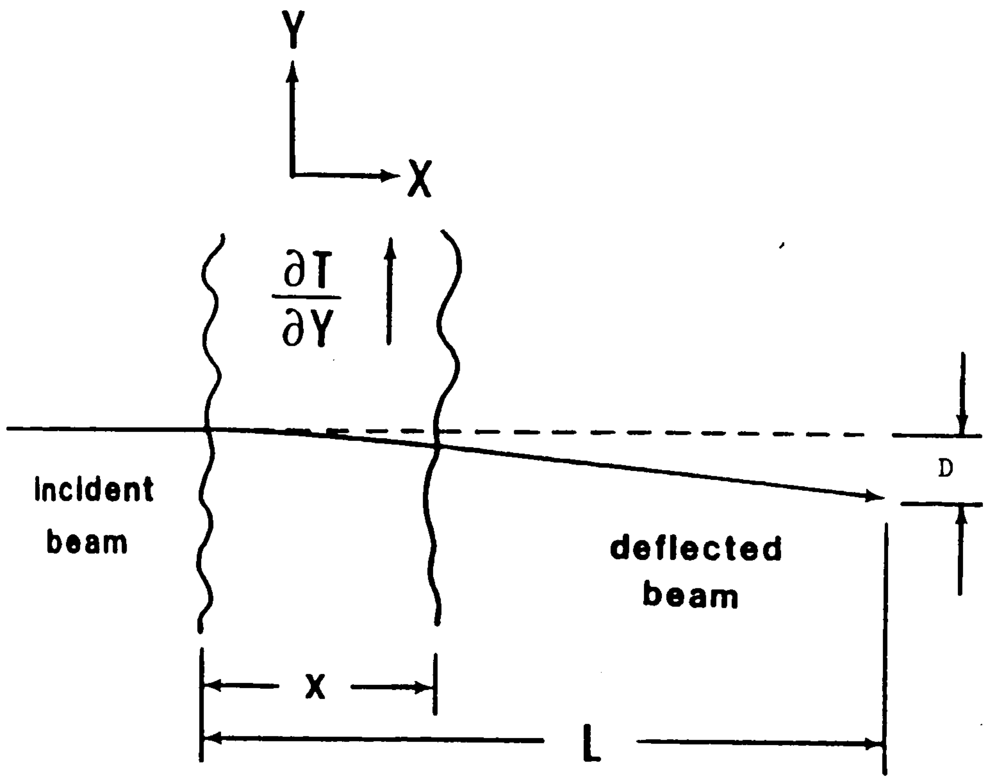

Figure 2. Schematic Diagram of Beam Steering, Where D is the Beam Deflection Over Total Pathlength L and the Traverse Temperature Gradient Occurs Over Distance X.

Single particle counters are useful for low number densities, where one particle at a time is in the optical probe sampling (control) volume. Single particle counters that measure the amplitude of scattered light have been used for years, often together with extractive sampling to determine individual particle sizes scattering that light. However, many light scattering methods used in single particle counter systems will not yield good results in an in-situ environment if the particle trajectories through the optical probe volume cannot be controllably aligned with the geometry of the probe volume. Also, for high particle number densities, methods using absolute light scattering intensity experience partical extinction of the laser beam before the light is scattered by the particle to be measured. Still, the main drawback with single particle counters is that, because of the Gaussian nature of a laser beam intensity profile across the beam, and no control of particle trajectories, the same measured scattering amplitude can result from a small particle passing through the center of the probe volume or a large particle passing through the edge. Hodkinson's method [3] developed by Hirleman, overcomes measurement ambiguities caused by lack of trajectory control by using relative intensity measurements in a ratio of scattered signals obtained at two optical collector system angles. The angles must be appropriate for the particle size range of interest, so that the ratio is a monotonic function of particle size. Even if appropriate angles are found, a problem exists because the two detectors of the optical signal collectors "see" somewhat different optical probe sampling volumes. Also, the detectors do not respond identically, because of intrinsic manufacturing and/or calibration differences, and their response variations have to be carefully evaluated in calibration for every pair of detectors used. Holve and Self [2,4,5] present a different method to account for particle trajectory variations on measured amplitude by collecting light over a large part of the forward lobe of the scattering intensity distribution and using a deconvolution scheme, together with a careful calibration procedure based on particles of known size, to provide a most probable size distribution. Holve [5] used an experimental calibration to give a most probable size distribution to account for the spatial variations of the light source and Son [6] addressed the problem by developing an analytical calibration.

One of the primary flow diagnostic tools that is based on small, single particle light scattering is the laser-Doppler velocimeter (LDV). LDV is a well developed, laser-based technique for measuring individual small particle velocities from the light scattered by those particles as they cross a laser beam. Cummings and Yeh [7] first used the Doppler shifted laser light scattered by moving objects as a tool in fluid flow measurement. Since then, laser Doppler velocimetry has been developed into a commonly used non-intrusive measurement technique. Because of the optical similarities to in-situ optical sizing arrangements, LDV can be used simultaneously with some of the in-situ particle sizing techniques. Obviously, if particle size-related laser light scattering characteristics can be coupled with an LDV signal analysis, simultaneous velocity and particle size measurements can be made. This not only would provide additional information during particle size measurements, such as particle size-velocity correlations, but would enhance LDV measurement uncertainties by allowing velocity samples to be qualified as being from the smallest particles, which are most likely to be in dynamic equilibrium with the fluid velocity, that is, they have velocities nearly equal to flow velocity and they respond quickly to fluid transients.

LDV was proposed by Farmer [8] for use as a particle sizer by showing that LDV signal "visibility" was related to particle size. Visibility was defined by Farmer as the ratio of the amplitude of the scattered LDV Doppler signal component to the mean value or pedestal of the LDV signal. Over a limited range of particle size, a monotonic relationship was predicted by Farmer between visibility and particle size. Farmer proposed to use this relationship to measure particle sizes. An LDV used for particle sizing and measuring velocity was labeled by Farmer as a particle sizing interferometer (PSI), and this nomenclature will be retained here. The basic PSI, like the LDV, consists of a source for a laser beam with a Gaussian intensity distribution (i.e., operating in the TEM_{00} mode), a beam splitter, transmitting and receiving optics, photo detector(s) and signal analyzer(s).

Since Farmer introduced visibility, signal characteristics other than visibility have been proposed for PSI designs. The most promising particle sizing characteristics proposed to date for use in PSI systems are scatter-intensity, visibility, and phase of scattered and collected light. Scatter-intensity, is essentially the amplitude of the scattered light, given by the product of scattering cross-section multiplied by $k^2/2\pi$, where k is the light wavenumber. The expected

PSI signal can be presented mathematically for a Cartesian coordinate system centered in the LDV probe volume, as shown in Figure 3, with the z axis bisecting the two input laser beams and the x axis in the polarization direction of the beams. The signal consists of a (relatively) slowly varying pedestal component, Ip, and a (relatively) rapidly varying Doppler component, Id, defined as:

$$I_p = \frac{C}{\pi b_0^2} \exp - \frac{2}{b_0^2} (x^2 + y^2 \cos^2\xi + z^2 \sin^2\xi) \cdot$$

$$P_1 \exp(- \frac{2yz\sin2\xi}{b_0^2})\sigma_{11} + P_2 \exp(\frac{2yz\sin2\xi}{b_0^2})\sigma_{22} , \tag{1a}$$

and

$$I_d = \frac{2C\sqrt{P_1 P_2}}{\pi b_0^2} \exp - \frac{2}{b_0^2}(x^2 + y^2 \cos^2\xi + z^2 \sin^2\xi) \cdot$$

$$\cos(\frac{2\pi y}{\delta} + \phi) \sqrt{Re^2(\sigma_{int}) + Im^2(\sigma_{int})}. \tag{1b}$$

The signal component labels "pedestal" and "Doppler" were initiated by Farmer [8] and are now generally accepted for describing LDV signals. In equation 1, C is a constant dependent on photodector gain and quantum efficiency, optics collection efficiency and signal processor gain. Also, ξ is the incidence half angle of the beams, b_0 is the beam waist radius, P_1 and P_2 are laser beam intensities, δ is the fringe period, ϕ is phase angle, σ_{11} and σ_{22} are scattering cross-sections of beams 1 and 2, and σ_{int} is the beam scattering interference cross-section. The exact expressions of σ_{11}, σ_{22} and σ_{int} are given by Pendleton [9]. Particle velocities are determined from the frequency of the I_d signal, i.e., from $\cos (\frac{2\pi y}{\delta}) + \phi$.

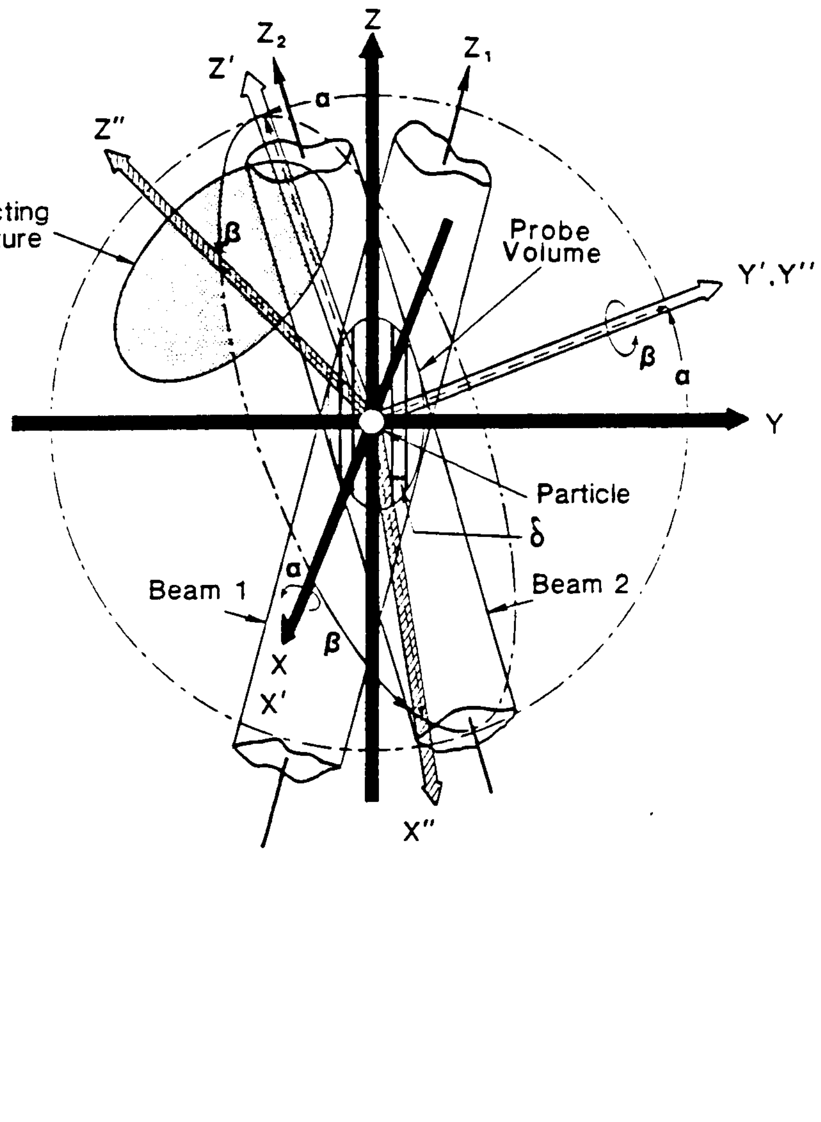

Figure 3. Coordinates of Optical Geometry.

Phase angle ϕ, called hereafter "phase", is defined as:

$$\phi = \tan^{1}\mu\{\mathrm{Im}(\sigma_{int})/\mathrm{Re}(\sigma_{int})\} \qquad (2)$$

As shown in Figure 4, the shape of the pedestal signal is the same as that obtained with a single laser beam. Thus, measurement of the peak or the averaged intensity of the pedestal signal (or for special cases, of the envelope of the Doppler signal) gives the scatter-intensity information. Visibility, as shown in Figure 5, is represented as the ratio of the peak or average intensity of the magnitude of the Doppler signal to the peak or average intensity of the magnitude of the pedestal signal, i.e.

$$|Ip| / |Id| \text{ or } |\overline{I}p / |\overline{I}d| .$$

Phase can be measured either as the phase difference between Doppler signals from two different photodetectors or as the time difference between Doppler and pedestal signal peaks. Figure 4 shows PSI signals with and without a phase shift.

The particle size range measurable with scatter-intensity is only restricted only by the output range of the signal processor, since the scatter-intensity increases continuously with particle size. The resolution depends strongly on the signal processor gain and the slope and monotonicity of the scatter-intensity versus size parameter curve. However, as seen in equation (1a), the peak intensity of the pedestal signal is a function of the x, y, z coordinates that define the particle trajectory and is subject to drifts in source intensity (P_1 and P_2) and system gain, C.

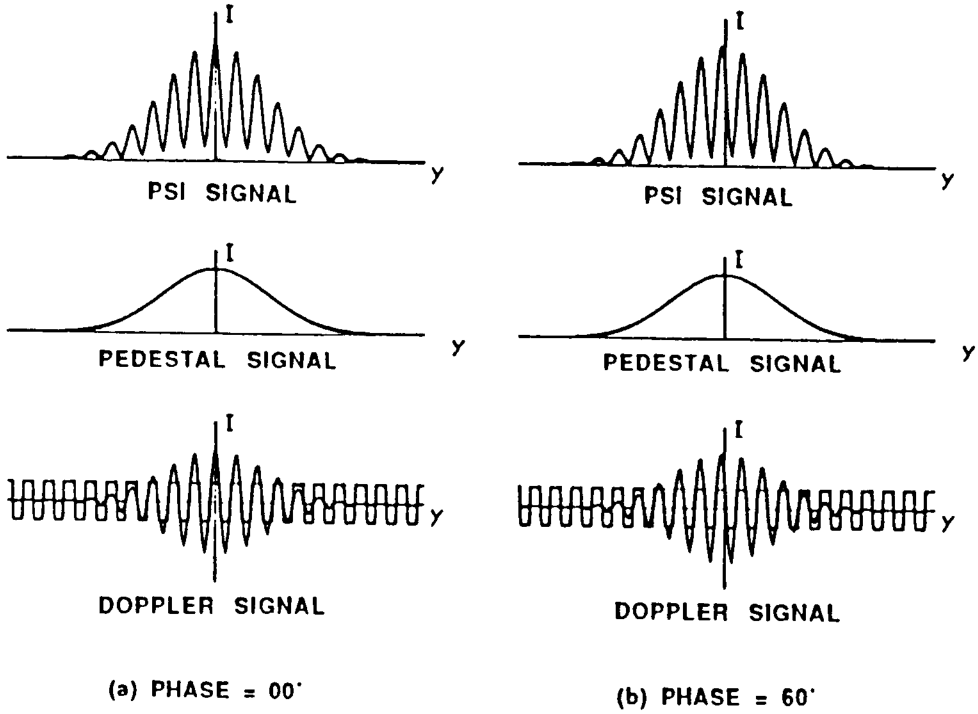

Figure 4. Composition of PSI Signal.

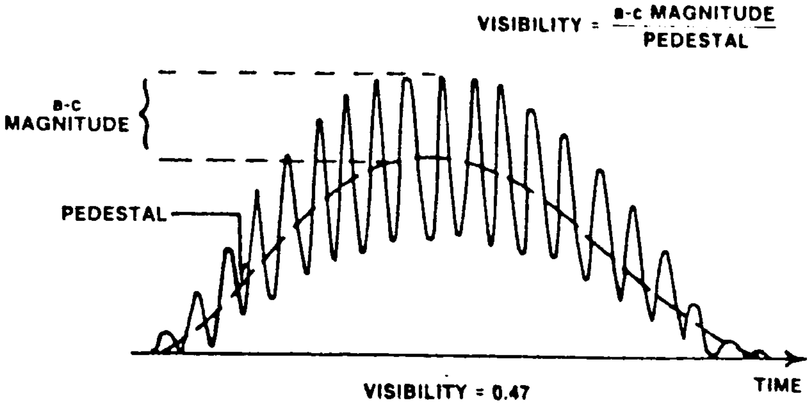

Figure 5. Visibility.

Because visibility is a ratio of Doppler-to-pedestal intensities, it is insensitive to system gain and temporal source beam intensity variations, but is still a function x, y and z and thus a function of particle trajectory. The possible visibility range is 0 to 1 and is associated with different particle size ranges depending on the collector geometry and fringe period. With different collector geometries and fringe periods, particle sizes of about 0.5 micron to several thousand microns are measurable. The maximum measurable particle size using the visibility method, increases with increasing fringe period; however, it is restricted by the signal processor capability. When the minimum visibility that can be resolved is 0.01, up to 100 discrete particle sizes can be resolved and as fringe period increases, size resolution decreases. Furthermore, because the slope of the visibility-size parameter curves is lower for smaller particles, visibility resolution is always less for small particles than for large particles.

The Doppler signal phase, d, has also been shown to provide a particle size measurement by Durst and Zare [11], Bachalo and Houser [12], and Saffman, Buchhave and Tanger [13]. As shown in equation (2), phase is independent of x, y and z coordinates that define particle trajectory. Also, phase, like visibility, is insensitive to system gain and illumination source intensity drifts, and has a measurable particle size range which is a function of fringe period. The particle size range measurable with phase is the same as with visibility [10].

Using PSI signal characteristics to determine particle size can give large uncertainties due to certain characteristics of the LDV scattered light. The scattering characteristics are highly non-linear and often non-monotonic functions of: index of refraction of the particle, and of the receiving lens size and location relative to the particle coordinates and incident beam directions. These effects are especially important for particle sizes less than 3 microns [10]. In particular, the amplitude and period of non-monotonic variations with particle size of the PSI signals obtained from the scattered light depend strongly on the size of the receiving lens, the location of the receiving lens and the fringe spacing (i.e., the PSI geometry). There are also uncertainties associated with drift in photodetector and signal processor gains, as well as temporal and spatial variations in the source light field.

To obtain a reliable measurement of particle size, it is necessary to find PSI geometries which yield highly monotonic relationships between the measured scattering characteristics and the particle size range to be measured, for the range of particle index of refraction encountered. To identify an optical system and its geometry which yields a highly monotonic scattering-to-size relationship, a complete experimental or analytical evaluation is needed of the geometric effects. Experimental evaluations are difficult to perform correctly, and the difficulty is compounded by the large number of possible geometric variations that have to be evaluated. Analytical evaluations have also been difficult to perform since the mathematical analysis is complicated and extensive computational time is required.

Particle sizing analysis can be divided into three particle size regimes; particles with diameters much less than the wavelength of light, with diameters greater than the wavelength of light, and with diameters comparable to the wavelength of light as suggested by Self [2]. Simple analyses are available for two regimes: the Raleigh analysis for very small particles of diameter less than 0.05 μm, and forward scatter diffraction analysis for larger particles, of diameters between 1 and 50 μm. Rayleigh scattering is used when the particle diameter is much less than the wavelength of the incident beam, i.e., when particle diameter is less than a twentieth of the wavelength of light [1]. For larger particles, where particle diameter is still less than the light wavelength, (e.g. macromolecules) the Raleigh-Gans approximation applies. This approximation requires that the light undergo only a small phase shift when passing through the particle, thus the particles must have a similar refractive index to their surroundings. Diffraction theory will provide reasonable estimates of the light scattering in the on-axis forward direction for particles with diameters greater than the wavelength of light. The lower particle size limit of diffraction theory is determined by the forward diffraction lobe which is very wide, about 35 degrees for small particles, which requires a large collection aperture. The upper limit is set for large particles when the lobe is narrow, about 1 degree, as the size at which significant interference will be experienced from the incident unscattered beam. However, as shown in Figure 6, analysis for the third regime, when particle diameter is comparable to

Intermediate Size - Mie Theory

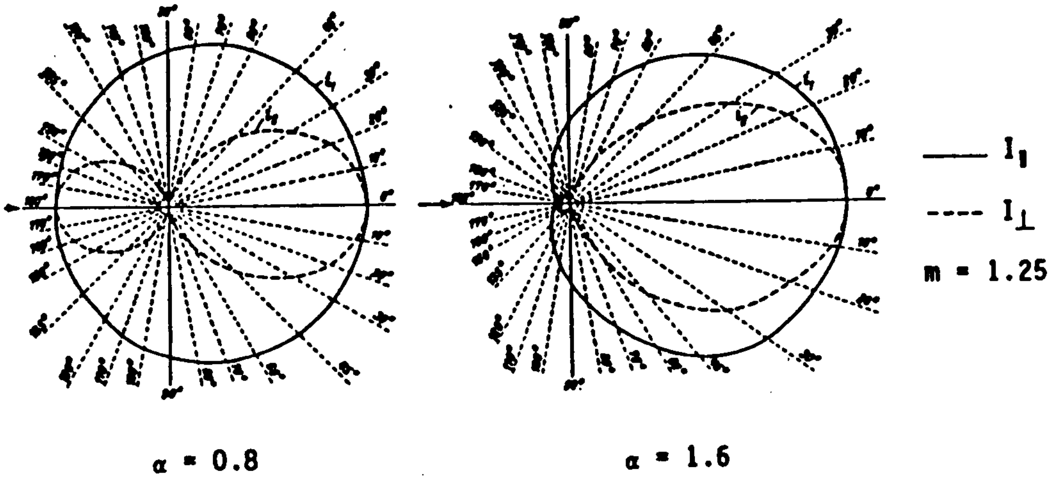

As α increases above 0.3, the scattering efficiency increases less rapidly than α^4 and the pattern becomes increasingly forward directed.

THREE REGIMES - Small, Intermediate and Large Particles

		For λ~0.5 μm
Small: Rayleigh limit simple analytic results	$\alpha \lesssim 0.3$	$d \lesssim 0.05$ μm
Intermediate: Full Mie Calculations necessary	$0.3 \lesssim \alpha \lesssim \frac{3}{m-1}$	$0.05 \lesssim d \lesssim 2\mu$
Large: Approximation as Diffraction + Reflection + Refraction	$\alpha > \frac{3}{m-1}$	$d \gtrsim 2\mu m$

Figure 6. Rayleigh-Mie Diffraction Regimes.

wavelength of the scattered light, full Lorentz-Mie scattering theory is essential to accurately describe the light scattering.

Of most interest in laser anemometry and particle sizing interferometry is the Lorentz-Mie region where particles are close to the wavelength of light. Fortunately, recent analytical developments of Mie analysis have simplified analytical evaluations for the PSI optical configuration. Specifically, Pendleton [9] developed a generalized Mie scattering solution for the PSI, to compare scattering characteristics for different geometries. Son [6] implemented Pendleton's mathematical development as an efficient computer code for detailed PSI analysis.

Prior to Pendleton's and Son's developments, approximate and/or simplified Mie solutions and scattering analyses were used to provide important evaluations of the different PSI particle sizing limitations. Robinson and Chu [14] presented a detailed analysis of single particle scattering characteristics in a cross-beam LDV based on scalar diffraction theory. They found that errors in determining particle sizing errors occurred when the collection aperture was too small and pointed out some limitations of the PSI as a particle sizing instrument. Included among these limitations is use of visibility when measured in the backscatter LDV collector optics arrangement, repeatedly varying from nearly 0 to 1.0 because visibility is highly non-monotonic, for this arrangement. Holve [4] used Mie theory computations to determine an optimal forward light-scattering geometry for sizing both spherical transparent particles and irregularly shaped light-absorbing particles in the range of 5 to 80 μm, using PSI visibility. Furthermore, the measurable visibility range corresponds to different particle size ranges, depending on the fringe period and collector geometry. Thus, by selecting different geometries and fringe periods, Holve showed that it is possible to measure particles up to several thousand microns diameter. However, for the larger size ranges, visibility is not a very sensitive measure of particle size since the variation of visibility remains constant at 1 to 0, or less.

Several researchers have identified problems associated with using amplitude (i.e. scatter-intensity) for particle sizing. These problems include sorting out variations in signal strength caused by both temporal and spatial variations of incident intensity. If a ratio of light intensities collected at different angles is used to avoid the problem of incident intensity variations, as proposed by Hodkinson [3] and implemented by Hirleman, the detectors see different probe volumes, and even when viewing scattering from the same particle, the two detectors do not respond identically to signal amplitude. As mentioned previously, Holve's [4] single detector technique for resolving the incident intensity variations only provided a most probable size distribution from the measured signal amplitude distributions, and suffers because velocity and size cannot be correlated. Since the visibility measure is a ratio of intensities, it is sensitive to system gain and temporal source beam intensity variations, and does not require multiple detectors for this ratioing as does Hodkinson's technique. However, as discussed previously, the accuracy of visibility, like signal amplitude, depends on the particles going through the central region of the probe volume. So visibility also depends on particle trajectory. Also, visibility works only for low number densities, (i.e., $<10^6/cm^3$) when used as originally proposed [15] in an on-axis forward scatter arrangement. Some improvement in the measurable number densities can be obtained with an off-axis arrangement, but when optical techniques are implemented to verify appropriate particle trajectories, these number density limitations become more restrictive.

LDV Doppler phase is the most recently proposed PSI particle sizing signal. As a particle sizing method, Doppler phase has several advantages. As mentioned previously, phase, being strictly a scattering cross-section phenomemon, is independent of particle trajectory. For example, because phase is not a function of the geometry of the probe volume, the same phase relationship is obtained regardless of where the particle crosses the probe volume. Also, phase, like visibility, is insensitive to system gain and source intensity drifts, and can be related to a particular measurable particle size range which is a function of fringe period [10]. Thus, phase measured with either two detectors or one detector has more advantages as a particle sizing quantity than any of the other proposed PSI particle sizing signals. Still, questions remain; how sensitive is phase to particle size; how monotonic is the phase-size relationship; and what are the effects of the optical geometry. A detailed collection is needed of measured or predicted Doppler phase variations with particle size, to answer these questions.

<u>Phase Sizing</u>

A Laser Doppler Velocimeter measures velocity by detecting the Doppler shift of light scattered from a particle moving in the flow. Direct detection of the Doppler shifted light can be performed, but an optical heterodyne detection technique is generally used based on processing the Doppler shift as a difference frequency between light from two sources. In the dual beam heterodyne detection method, the scattered light from two incident beams ($\hat{S}_1$ and $\hat{S}_2$) is heterodyned. The dual beam LDV arrangement has many advantages including: 1) it is the easiest system to align; and 2) the Doppler frequency is independent of the location of the collection optics, depending only on the velocity component in the plane of the beams and normal to their bisector, so large collection apertures can be utilized without creating Doppler frequency ambiguity.

The fringe model of the dual beam system is a convenient way of visualizing how an LDV works. The basic non-frequency shifted, dual beam LDV or PSI is shown in Figure 7. The laser beam is split into two beams which are then refocused and crossed, forming a crossover region or ellipsoidal probe volume. The surface of the ellipsoid is defined by the spatial points where the amplitude of the Doppler signal is $1/e^2$ of its centroidal value. Since the two laser beams were developed from one initial beam, they are coherent in terms of their axial and traverse wave characteristics, so they form alternating constructive and destructive interference planes on a detector placed in the probe volume. The bright and dark patterns, called

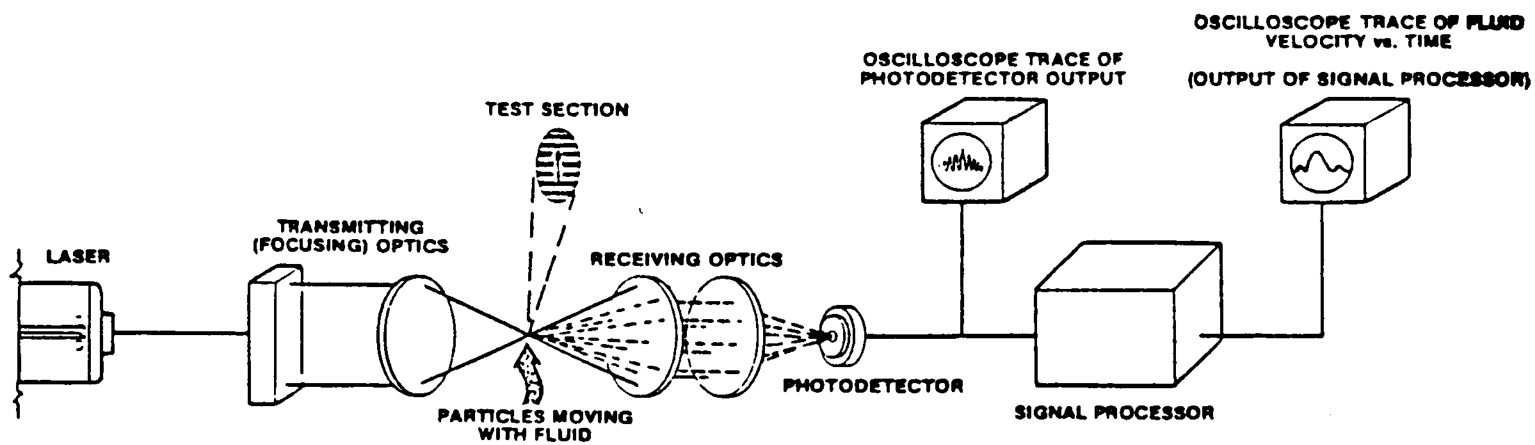

Figure 7. Complete Dual Beam and PSI System.

maxima and minima respectively, define the fringe spacing as the distance between adjacent maxima or minima. This fringe spacing, δ, is determined solely by the geometry of the optics and the laser beam wavelength, λ, as:

$$\delta = \frac{n\lambda}{2\sin k} \tag{3}$$

where n is the index of refraction of the fluid and 2k is the angle between laser beams. A particle moving in the fluid stream will scatter light when it traverses the probe volume. The light scattered by the particle into an aperture is focused on a photomultiplier tube (PMT) which sends a signal to a signal processor. As defined previously, the signal has a rapidly varying AC component superimposed on a slowly varying DC or pedestal component. Figure 8 shows how the light intensity in the probe volume varies depending on where the particle crosses the region. The angle k is also illustrated in Figure 8.

Since u, the particle velocity, is generally much less than the velocity of light, the velocity-frequency relationship for the light scattered is given by

$$f_D = i/\ (\hat{S}_1 - \hat{S}_2) = 2\ u_x\ \sin k/\lambda n = \frac{u_x}{\delta} \tag{4}$$

since $|\hat{S}_1 - \hat{S}_2| = 2 \sin k$ and $u_x = |u| \cos a$, where a is the angle between the velocity vector and the x component.

LDV signal phase was first applied to particle sizing by Durst, et al. [11], for the measurement of large refracting particles using two detectors located in off-axis forward and backward directions. Use of LDV signal phase for particle sizing has been developed by

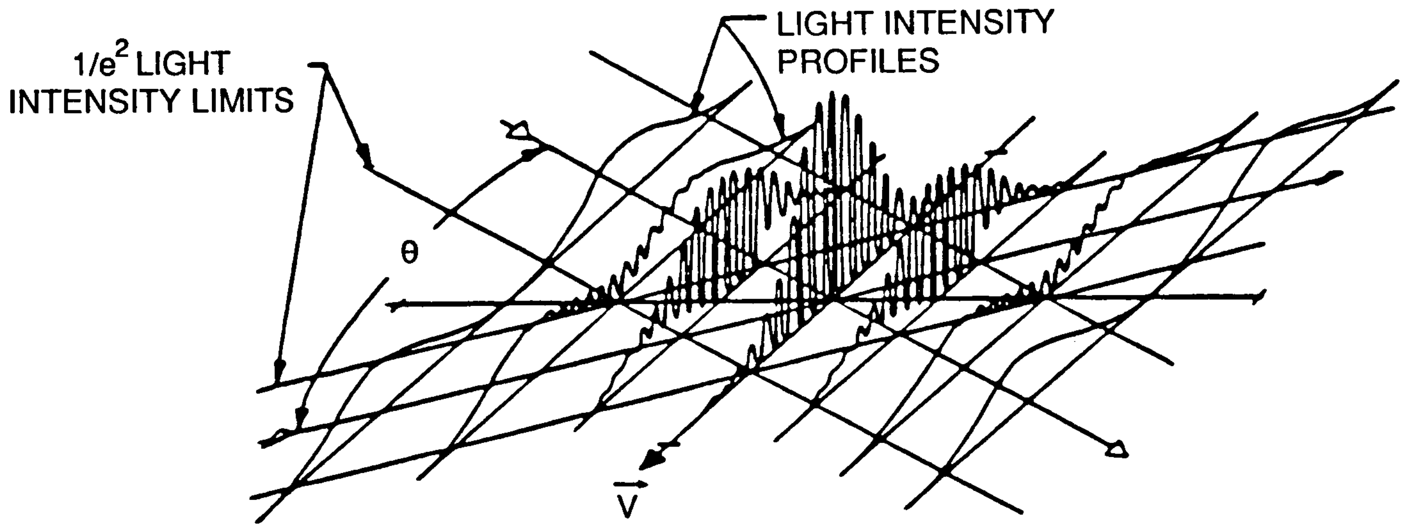

Figure 8. Signal Characteristics Along Measuring Volume.

Bachalo et al. [12] and Saffman et al. [13]. Bachalo and Houser developed a phase/Doppler spray analyzer technique to measure the "spatial frequency" of the scattered fringe pattern by using two or more detectors separated by fixed fringe spacings. When the particle passed through the LDV laser beam crossover region, (i.e. the probe volume), the fringe pattern appeared to move past the receivers at the Doppler difference frequency. A Doppler burst signal was produced by each detector but with a phase shift between them. The phase shift was determined by measuring the time between the zero crossings for the signals from detectors 1 and 2, τ_{1-2}, and dividing by the measured Doppler period, τ_D. Therefore

$$\tau_{1-2} = \frac{\tau_{1-2}}{\tau_D} \times 360° \tag{5}$$

where the measurements were averaged over all cycles in the Doppler burst signal. The phase shift was then related to particle size using geometrical optics theory. Both off-axis forward scatter and back scatter light detection was used by Bachalo and Houser and gave an overall size range of 3 to 2000 microns or greater for spherical particles. They suggested that their method may be valid for drops as small as 0.5 μm, but indicated that a full Mie scatter analysis, such as that developed by Pendleton [9,16], would be necessary to prove this. Bachalo's analysis was performed for the dual beam LDV configuration for large off-axis receiver angles, and in doing so he was able to reduce the measurement region by as much as two orders of magnitude compared with the on-axis receiver location methods, as typically used for visibility. This introduced the possibility that even in relatively dense sprays, the size and velocity of individual particles could be measured.

Simultaneously with Bachalo's developments, Buchhave et al. [13] developed a method of optical size measurement based on detection of phase of the Doppler signal from a dual beam or fringe mode laser Doppler anemometer or LDA. Saffman, Buchhave and Tanger [13] described an application of this instrument to measure air bubbles from 5 to 150 microns in diameter in water flows. According to Saffman et al., with a proper geometry, the phase difference between signals from two detectors, at different scattering angles, is linearly related to particle diameter. Also, this instrument uses three detectors, so that large phase differences for one pair of detectors gives a smaller phase difference for another pairing. Thus phase differences greater than 2π radians can be distinguished. A fourth detector was also used so that non-spherical particles can be identified. However, Saffman et al. only claim to be able to determine size for spherical particles. Spherical particle concentrations can also be measured using the LDV phase technique. Saffman described the dependence of the instrument's measurement cross section on particular diameter allowing the measurement of particle concentration to be made [13].

Saffman, et al, analyzed the phase-size LDV signal relationship using a geometrical optics approximation. Diffraction, refraction and reflection each contribute separately to the scattered radiation in this analysis. Saffman, et al, neglected diffraction since they were interested in scattering at large off-axis angles. Saffman et al showed that their experimental results were in excellent agreement with their geometrical optics theory, down to a particle diameter of 5 microns. Their results for various sized collection lenses show that oscillations in the phase-size curves can be effectively damped out by increasing the size of the collection aperture. They suggest it is possible to extend the measurements to less than 5 microns. By using 3 detectors, the phase shift can be unambiguously measured until the phase shift for the least sensitive detection pair crosses 2π radians. This method of measuring phase shifts greater than 2π radians for the more sensitive pair provides for a very wide dynamic size range as well as high resolution.

Purpose of Research

At this time, a collection of detailed experiments or light scattering predictions of phase does not exist. As just indicated, only one scattering prediction curve has been developed using a combination of reflection and refraction theory, and verified by using air bubbles in water. A few other experimental calibrations have been done with different particles by Bachalo and Houser [12] but their theoretical analysis was performed using geometrical optics theory for both off-axis forward scatter and back scatter light detection, with only a few selected geometries. The purpose of this project is to provide extensive, full Mie predictions of the phase-size relation, particularly for the 0.3 to 6 μm size range, for numerous collector optics geometries, numerous particle indices of refraction, two incident laser beam polarizations, several fringe spacings, and two different incident wavelengths. These predictions are generated for fine variations in particle size, to allow assessment of the variability (and possible oscillations) of the phase-size curves. From these predictions it is possible to select optical geometries for optimum response, which includes optimization of receiver location(s) and size(s) for the measurement size range of interest and the measurement particle index of refraction range of interest. If the number of detectors to be used is defined, the results allow the range of applicability to be established, and the maximum attainable resolution and sensitivity of the instrumentation used to be specified.

CHAPTER II

MIE SCATTERING THEORY

Mie [17] applied Maxwell's equations to formulate the boundary value problem describing the scattering of electromagnetic waves when a plane polarized wave is incident on a homogeneous sphere. Mie solved the problem by constructing an infinite spherical harmonics series expansion of the incident and scattered waves, where solutions in spherical coordinates result in a linear series of Ricatti-Bessel functions and associated Legendre polynomials. The boundary conditions are used to evaluate the series coefficients. The resulting scattered electromagnetic field is given as a function of the size parameter ($X = \pi d/\lambda$), where d is the diameter of the scatterer and λ is the wavelength of the incident electromagnetic wave. In addition, the scattered field is a function of the scattering angle, measured from the forward direction; the complex refractive index, of the medium; and the polarization of the incident wave, defined as either the E vector parallel or perpendicular to the plane of observation [2].

Mie theory results provide prediction of the scattered electromagnetic field at a point. To determine the scattered light collected by an aperture, an integration of the Mie solutions over the points defining the aperture are required. This further complicates Mie analysis, and greatly increases the numerical computation time required for Mie theory analysis. Diffraction and refraction theories can provide good results for restricted aperture locations where the scattered field is adequately described by one of these theories, but a big advantage to Mie theory is that it is applicable to all aperture locations and may be used to determine limits for possible application of refraction and diffraction theories [16]. A disadvantage of computer codes based on Mie theory is the often prohibitive cost of the extensive computer time required, since solution time is compounded by the necessity to calculate the scattered field for two beams when the dual beam LDV is used. However, no theory has yet rivaled Mie theory for scatter to an aperture centered in the backward hemisphere [16], and Mie theory, of necessity, must be used to provide these predictions. The most common LDV optical configuration is the backscatter configuration. Thus, Mie theory was selected for this analysis of LDV Doppler phase for particle sizing.

More Efficient Mie Algorithms

Dave [18] in 1968 pioneered the implementation of computer code applications for determining parameters of electromagnetic radiation scattered by a sphere. Wiscombe [19] in 1979 used a vectorized computer code for faster Mie scattering calculations. However, the additional numerical integration of the Mie solutions across the collection aperature (or lens) were still required, and solutions need to be generated for two beams which are crossed in dual beam LDV or PSI systems. Fortunately, an exact form of the Mie scattering solution for the light energy scattererd into a finite solid angle was given by Chylek [20] for a single beam, and Chu and Robinson [14] for two coherent beams. Both of these solutions are only applicable to the special cases of calculating total scattering, on-axis backward scattering or on-axis forward scattering. However, Pendleton [16,21] recently derived a Mie-scattering solution for the problem of simultaneous scatter from two or more coherent beams by generalizing Chu and Robinson's approach using angular momentum theory [22]. Pendleton used Euler angle rotations of the coordinates of each beam to make the beam propagation direction coordinates coincident with the coordinates defining the position of the circular collecting lens. Thus, the scattering calculation over a circular aperture located in any orientation relative to the beam propagation direction becomes the same as that for on-axis forward or backward cases.

Pendleton's solution can be applied to calculate phase, visibility and scatter-intensity for any particle size and for any circular collecting aperture location relative to the scatterer and beam propagation directions. Thus, Pendelton developed the theory for obtaining the spatial response of particle scattering characteristics without resorting to numerical integrations. However, the solution consists of a series of sums of products of associated Legendre polynomials, which often still require considerable computational time for evaluation. Son and Giel [23] provided improved methods for computer evaluation of Pendleton's solution, and provided limited results for LDV visibility and scatter-intensity vs. particle size, for a few specific indices of refraction and a couple different optical geometries.

Using Pendleton's Mie algorithms, while developing the improved computer evaluation methods [23], Son [6] investigated the PSI for sizing particle smaller than 3 microns. Son proposed simultaneously measuring peak amplitude of the pedestal signal, averaged amplitude of the pedestal signal, number of Doppler signal cycles, and signal visibility to improve the PSI measurements. Son used Pendleton's Mie scattering solution to find collection optics configurations which yielded a monotonic relationship between particle size and scattering intensity, and between particle size and visibility. Then an experimental investigation was conducted using a 50° off-axis forward scatter optical arrangement with an effective f-number 1.0 collector, since this arrangement provided a monotonic relationship for particle diameters up to 10 microns with a particle size increment of 0.15 microns. Particle size distribution measurements made simultaneously using the four different signal components were found to be consistent with the Mie predictions.

The approach taken for the purpose of this research was to use the UTSI developed Mie Code, incorporating Pendleton's solution [21] and Son's algorithms [23] to provide extensive predictions of the variations of the LV signal characteristics for a range of particle sizes, range of indices of refraction, and range of optical configurations. Because of the need for greater computer speed to reduce CPU requirements, the code was installed at the Computer Center of Excellence located on the campus of The University of Tennessee Chattanooga, on an IBM 4381 level 2 system. Response curves for the 0.3 to 6 micron size range were generated, with fine segmentation between points on the curves in the 0.3 to 6 micron range, taking into account of particle light scattering characteristics as complex functions of: particle size and index of refraction; the light wavelength intensity and polarization, and the location and response characteristics of the detector optical and electronic systems [24].

Description of Mie Code

Solutions for the generalized and conventional Mie scattering problem differ in the evaluation and calculation of the associated Legendre polynomials. Pendleton showed that these polynomials are generated by recursion relations, where the higher-ordered terms can be neglected thus allowing convergence [9]. As particle size increases, important considerations are determining the total number of terms necessary to minimize error and attain convergence and then evaluating these polynomials with the appropriate minimum error. A similar problem arises in evaluating the Mie scattering coefficients. Since convergence of the Mie scattering solution is highly dependent on the covergence of Mie scattering coefficients, the maximum number of terms to be evaluated is determined by the convergence criterion of the Mie scattering coefficients. Two schemes for evaluating Mie scattering coefficients are upward recurrence, from lower to higher order terms, and downward recurrence, from higher to lower order terms.

The upward recurrence method needs the least amount of storage and CPU time, but fails when the imaginary part of $Xm = 2\pi\ Dm/\lambda$ reaches a critical value, which is implemented in the code [23], determining when to shift from upward recurrence to another method. The downward recurrence method requires more storage and CPU time than the upward recurrence method but it is more stable than upward recurrence [23]. Therefore, the choice of an evaluation scheme depends on the real and imaginary parts of Xm. Wiscombe [19] and Dave [18] give an emperical formula for determining which scheme to use, since there is no fixed value of the real and imaginary parts of Xm. However, as the real part of the index of refraction, m, approaches 1, the stability of the downward recurrence method deteriorates, and Lentz's method [25] is more efficient than the downward recurrence method.

CHAPTER III

RESULTS

Determining particle size from PSI signal characteristics can result in large uncertainties due to the following characteristics of collected scattered light:

1) The collected scattering characteristics are functions of the index of refraction of the particle, and of the receiving lens size and location relative to the incident beam directions, especially for sizes below 3 μm.
2) The collected scattering characteristics are generally oscillating functions of particle size. The amplitude and period of oscillation depend strongly on the location and size of the receiving lens.

Therefore, for reliable particle size measurements, optical geometries must be found which show a sufficiently monotonic relationship between particle size and the measured scattering characteristics over the particle size range and index of refraction range of interest.

The UTSI Mie code was used to identify geometries which show sufficiently monotonic relationships between particle size and Doppler phase angle for reliable particle sizing. Variations in the phase versus particle size relation with particle index of refraction, m, effective collector f-number, FN collector coordinate system rotation angles, α and β, fringe spacing, δ, and two different laser beam polarizations, were calculated. Calculations were performed for indices of refraction of .7496, .8379, 1.1, 1.334, 1.592, 1.7, 2.0, 2.5, 3.0, and 3.5; FN values of 1, 2, and 4; α values of 0.0 to 75° in 5° increments; β values of 0 to 180° also in 5° increments; δ values of 5 and 10 μm; and polarizations with $\vec{E}$ and $\vec{H}$ parallel to the x-axis ($\vec{E}_x$ and $\vec{H}_x$, respectively). Most calculations were for a helium neon laser wavelength, λ, of 6328 Angstroms, though other wavelength calculations were performed, including argon-ion wavelengths of 4880 and 5145 Angstrons. However, wavelength changes affect the size parameter, only altering the particle size range applicability of the results. Thus effects of wavelength variations do not need to be presented.

The UTSI Mie code results are best presented graphically. The graphed results were obtained using the SASGRAPH plotting routine with the Tektronix 4107 terminal, Tektronix 4692 plotter, and IBM 4381 level 2 computer, at the University of Tennessee Chattanooga Computer Center of Excellence.

Figures 9 through 12 show the variations in Doppler phase for different indices of refraction with β being varied from 25 to 65 degrees in the different figures. Other parameters held constant are FN = 1, α = 35°, δ = 5 m, λ = 6328 Angstroms and an $\vec{E}_x$ polarization. Figure 9, for β = 25°, shows sudden jumps in phase accompanied by phase polarity changes, at different size parameters for all the different indices of refraction. Figure 10, for β = 45°, shows sudden jumps in phase only for m less than 1.73, while Figures 11 and 12 for β = 55 and 65°, show no jumps in phase for the particle size parameter range of the calculations. Thus, the occurrence of sudden jumps in phase accompanied by phase polarity changes, diminish with increasing

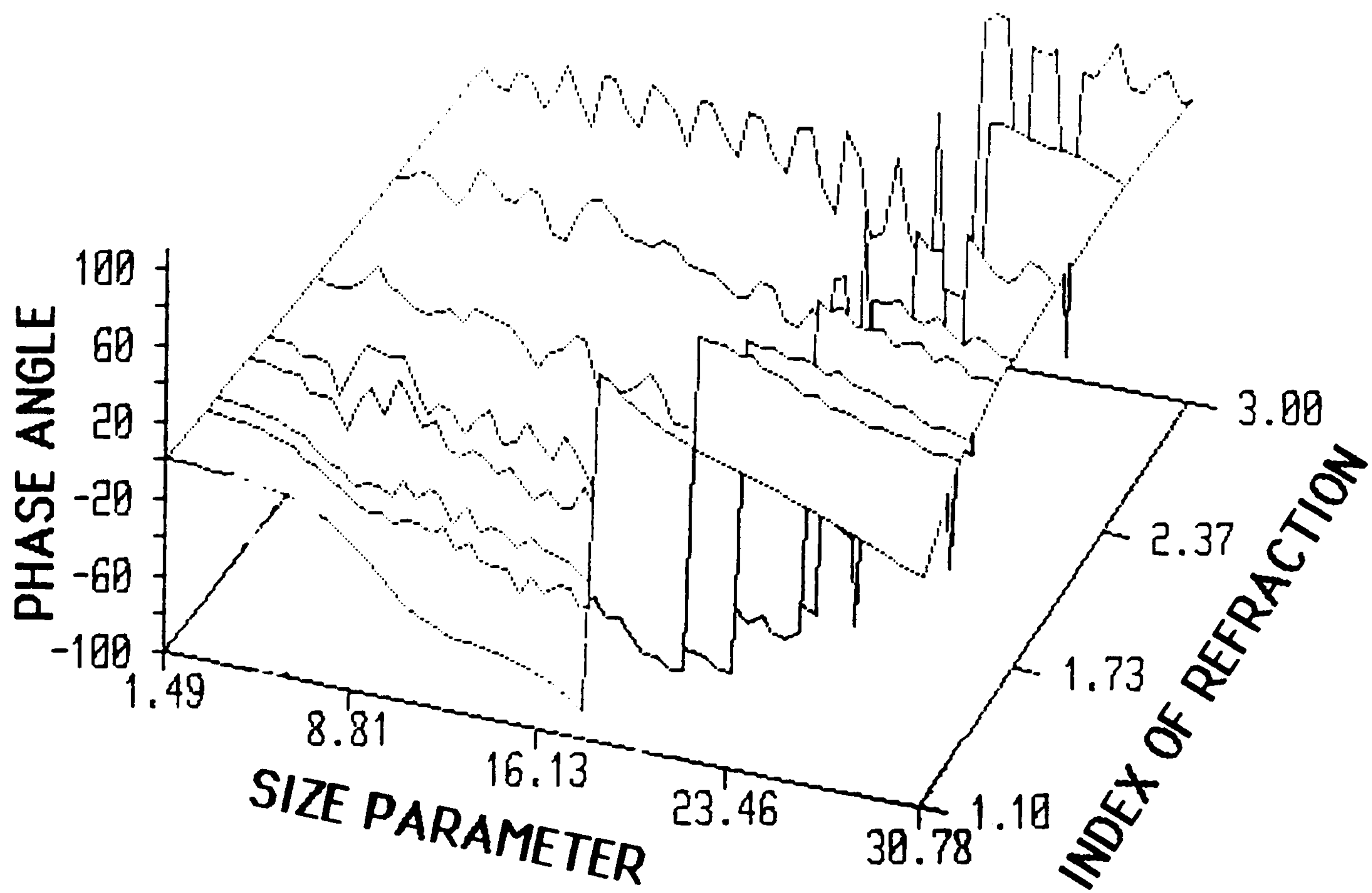

Figure 9. Phase Variation:
$\beta = 25°$, $\alpha = 35°$, FN = 1, $\delta = 5\ \mu m$, $\vec{E}_x$.

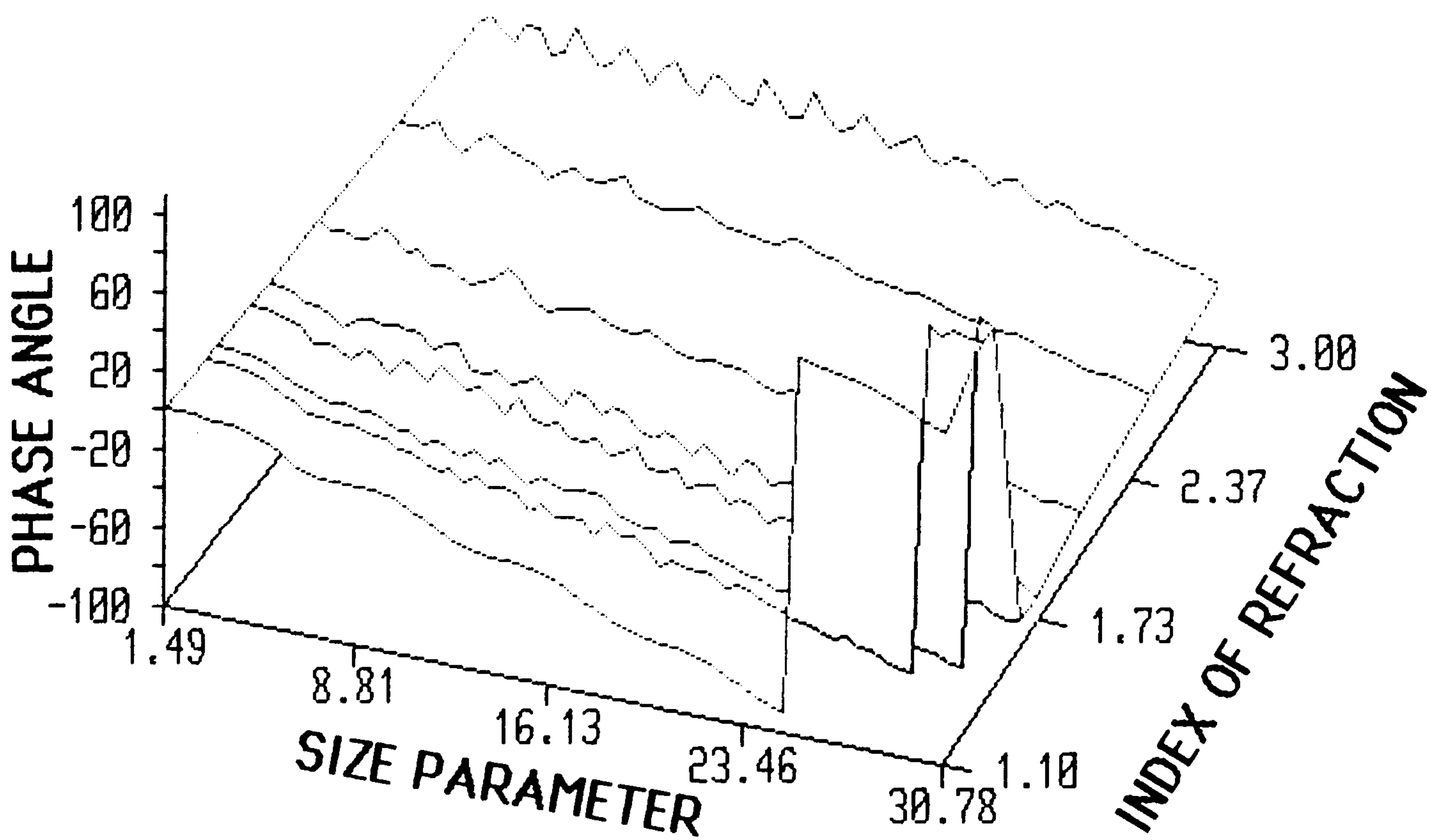

Figure 10. Phase Variation:
$\beta = 45°$, $\alpha = 35°$, FN = 1, $\delta = 5\ \mu m$, $\vec{E}_x$.

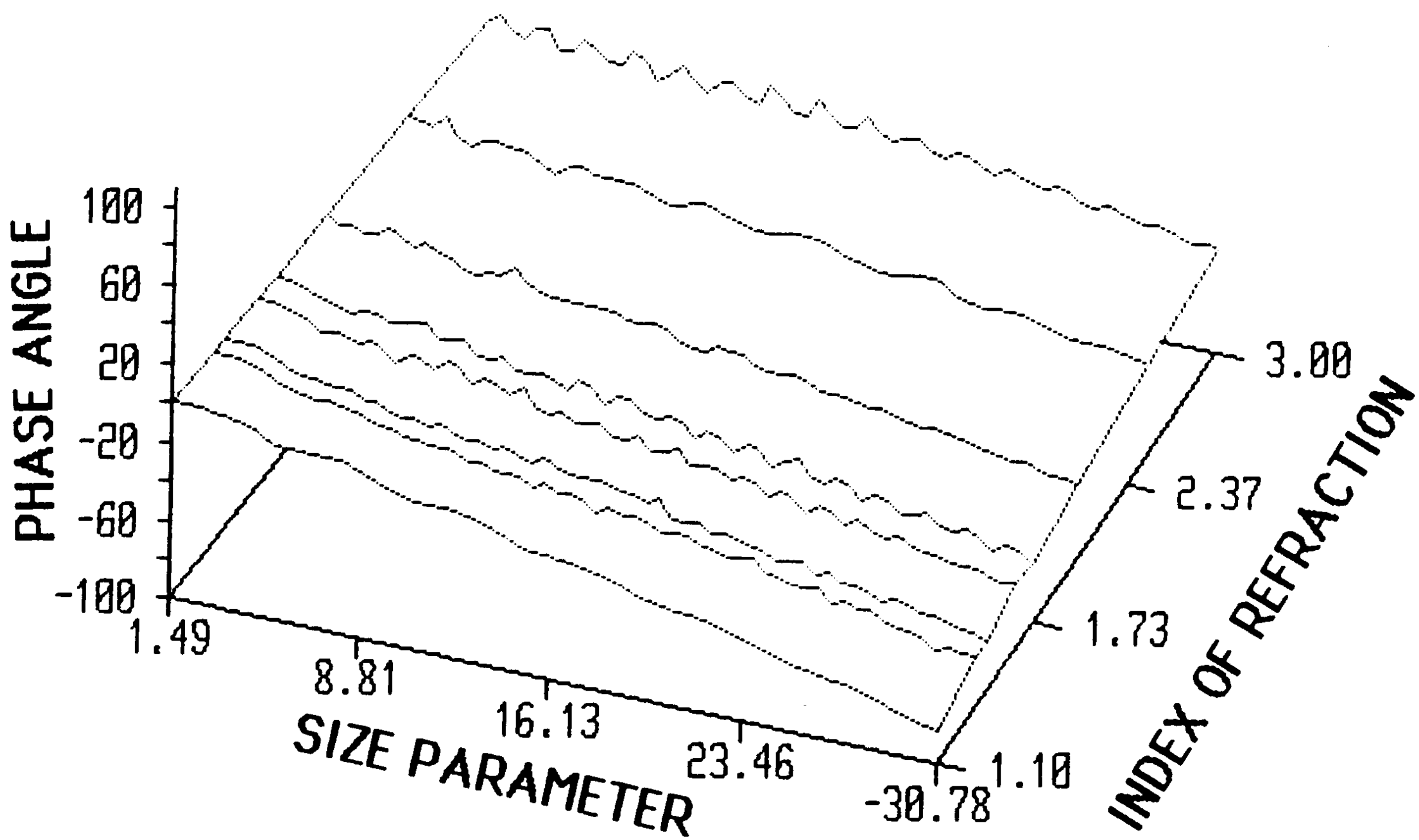

Figure 11. Phase Variation:
$\beta = 55°$, $\alpha = 35°$, FN = 1, $\delta = 5\ \mu m$, $\vec{E}_x$.

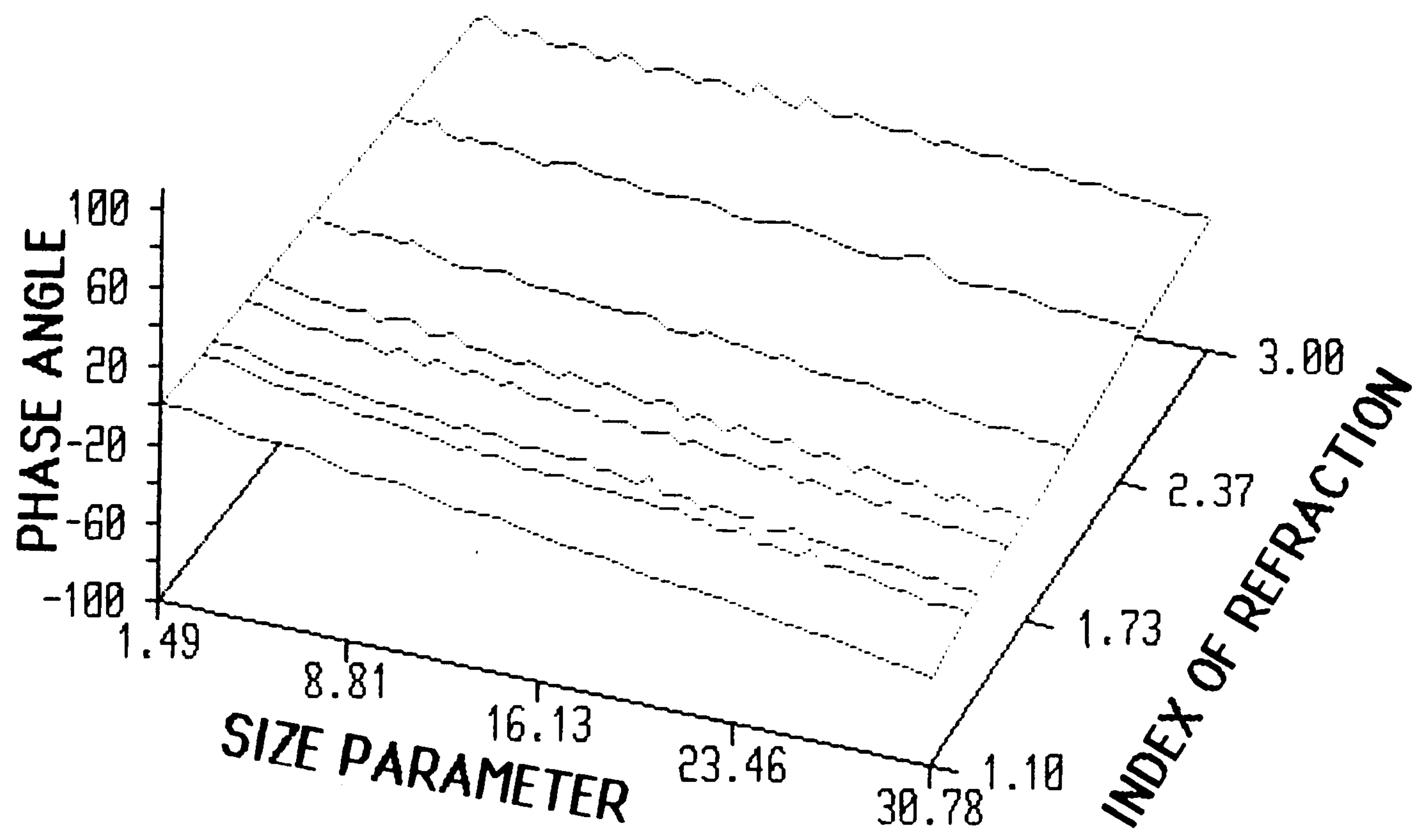

Figure 12. Phase Variation:
$\beta = 65°$, $\alpha = 35°$, FN = 1, $\delta = 5\ \mu m$, E_x.

β. As β increases from 25° to 65° the size parameter range before the jumps also increases, increasing the measurable size range, but the variation in phase with size parameter decreases so the measurement sensitivity decreases. As β increases the magnitude of the non-monotonic variations in the phase angle with increasing size parameter also decreases. So, although the sensitivity tends to decrease, the measurement uncertainty might increase as β increases from 55 to 65°. The $\beta = 0°$ case shown in Figure 13 shows multiple phase jumps and polarity changes and thus yields no size information. Figure 14 shows similar multiple phase jumps and polarity changes for different α's of 35°, 45°, 55°, and 65° with a constant particle index of refraction of 1.1. Again, there is no size information available for β's of 0°.

The effects of varying α are shown in Figures 15 and 16 for $\beta = 55°$ and $\beta = 70°$ respectively for a water droplet ($m = 1.334$). Other parameters held constant are FN = 1, $\delta = 5$ µm, $\lambda = 6328$ Angstroms, and $\vec{E}_x$ polarization. As seen in Figure 15, phase jumps occur for $\beta = 55°$ for α values greater than 45°, but as α decreases, the sudden phase jumps occur at larger size parameters. Phase jumps that appear in Figure 15 do not appear in Figure 16 due to the increase in β from 55 to 70°. However, as shown in Figure 15, and more clearly in Figure 16, sensitivity of phase to particle size parameter decreases as α decreases. These effects are opposites of the effects observed with β changes. Increasing β increased the measurable size range and decreased sensitivity while decreasing α increases the range and decreased the sensitivity. Effects of decreasing α to 0°

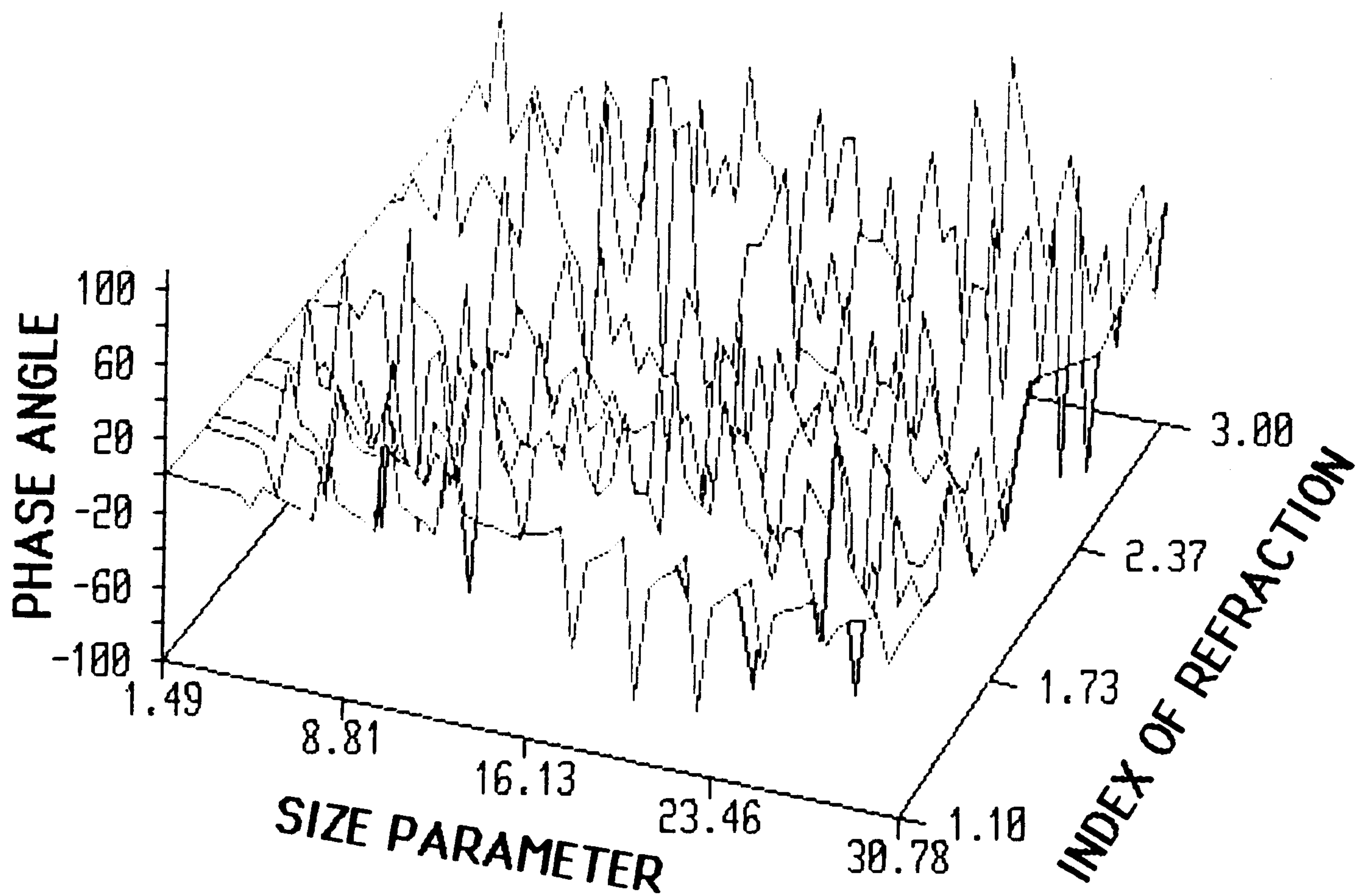

Figure 13. Phase Variation:
$\beta = 0°$, $\alpha = 35°$, FN = 1, $\delta = 5\ \mu m$, $\vec{E}_x$.

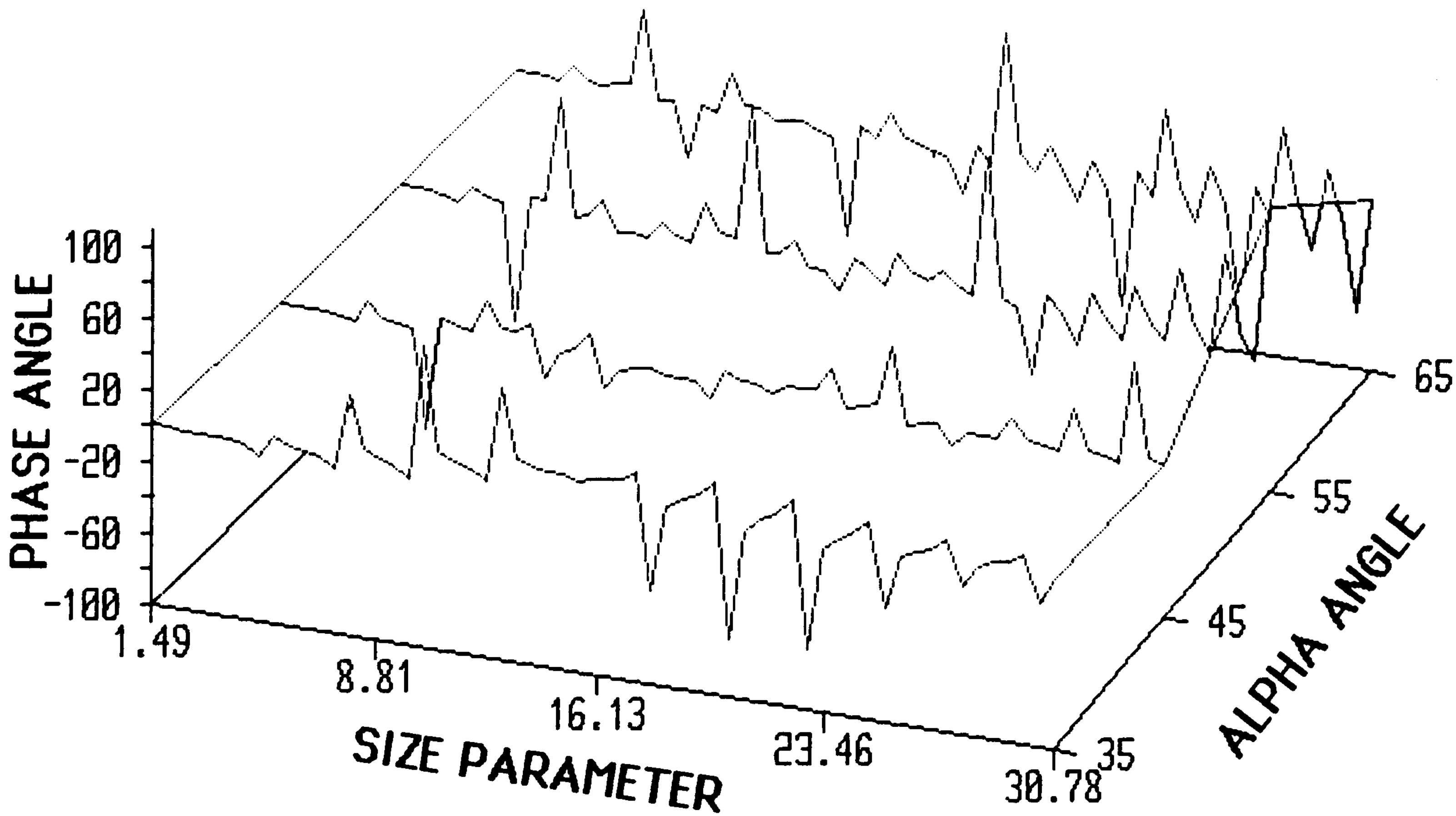

Figure 14. Phase Variation:
$\beta = 0°$, $\alpha = 35°, 45°, 55°, 65°$, FN = 1,
$\delta = 5\ \mu m$, $m = 1.1$, $\vec{E}_x$.

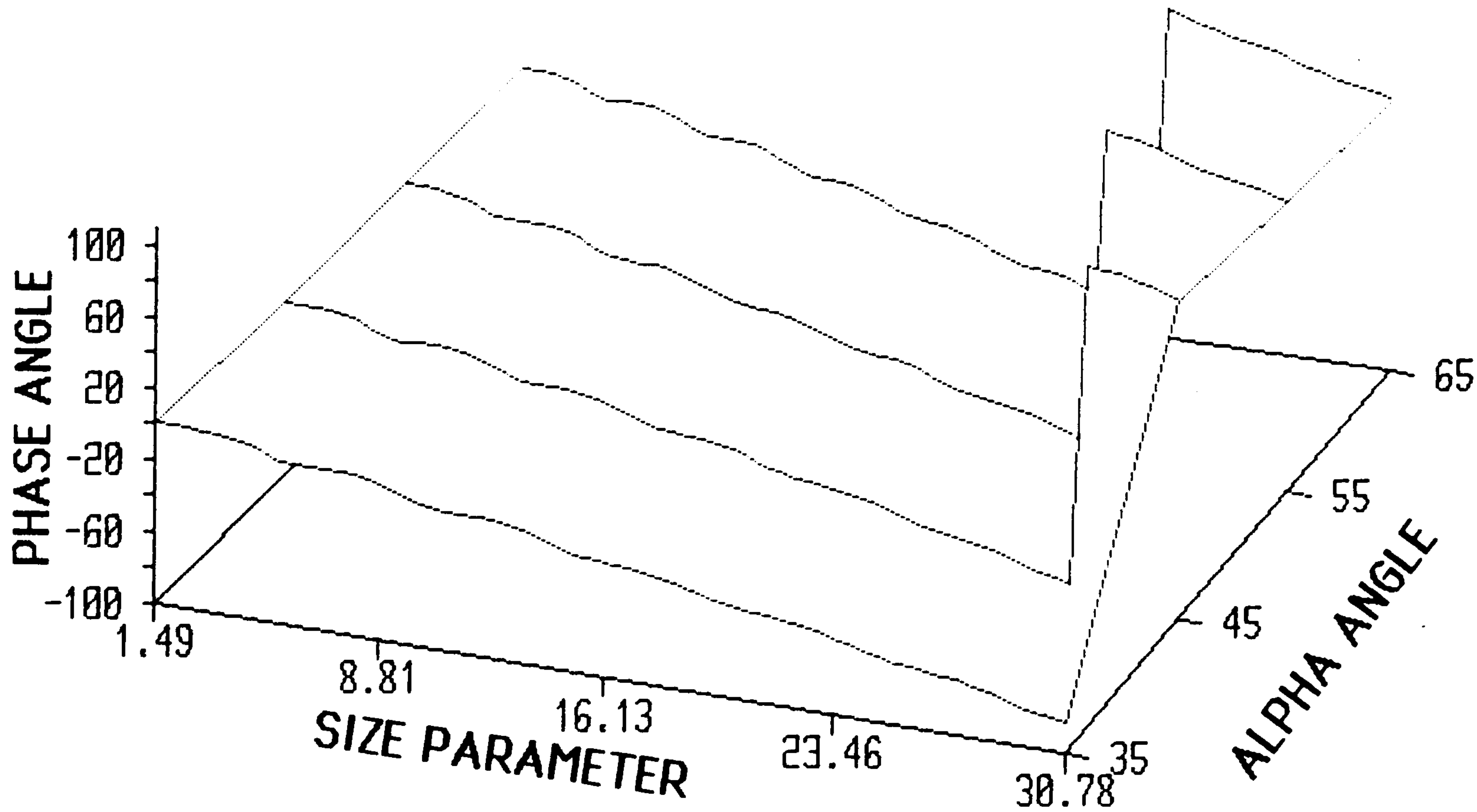

Figure 15. α Effects: $\beta = 55°$, $\alpha = 35°, 45°, 55°, 65°$, FN = 1, $\delta = 5\ \mu m$, $m = 1.1$, $\vec{E}_x$.

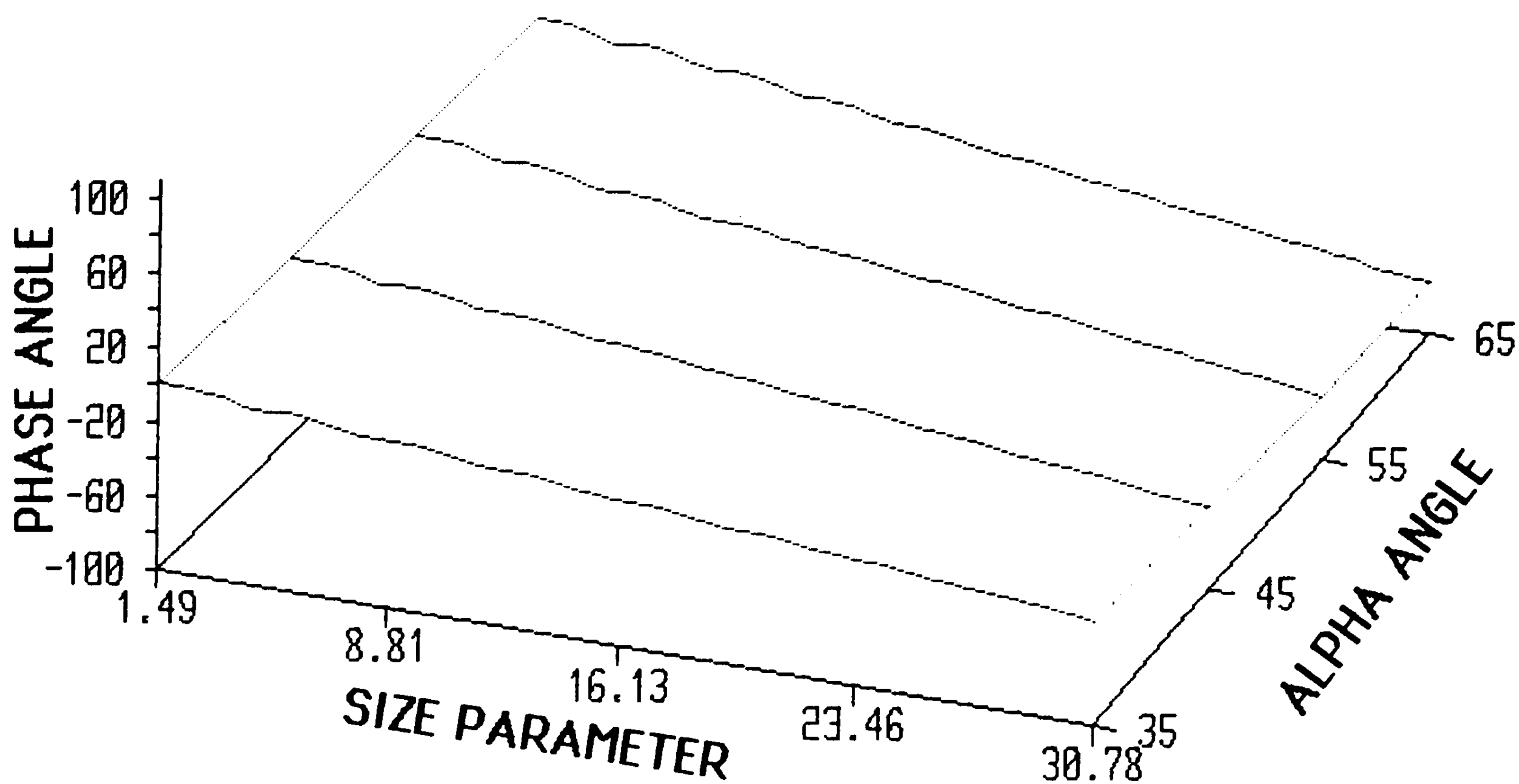

Figure 16. α Effects: $\beta = 70°$, $\alpha = 35°, 45°, 55°, 65°$, FN = 1, $\delta = 5\ \mu m$, $m = 1.1$, $\vec{E}_x$.

is shown in both Figures 17 and 18 for various β and m values, respectively. Both figures show that when $\alpha = 0°$ there is no phase change, and thus no size information.

Figures 19 and 20 show the α effects for an increased index of refraction (m = 2.5) from that shown in Figures 15 and 16 (m = 1.1). The increase in the index of refraction shifts the phase jumps to larger size parameters, decreases the sensitivity of phase to particle size parameter, and also increases the magnitude of non-monotonic response curve variations. Index of refraction effects are better shown in Figures 21 through 24, for β values of 35°, 55°, 55°, and 65° and α values of 15°, 15°, 45° and 45°, respectively. Parameters held constant are FN = 12, $\delta = 5$ μm, m = 1.1 through 3.5, and $\vec{E}_x$ polarization. Together these figures show that for constant α, as β increases, the phase size curves become smoother, with both a decrease in the magnitude and number of non-monotonic variations in phase with increasing size parameter. As shown in Figures 23 and 22, for a constant β, decreasing α from 45° to 15° results in a smoother phase versus particle size relationship also. As before, as α increases, must increase to get the same measurable size range and sensitivity.

Figure 25 shows the effects of varying FN for an index of refraction of 1.1. Both the magnitude and the number of non-monotonic variations in phase decrease as FN decreases, while the slope (i.e., the sensitivity) of the phase-size curves increases. Thus, the size measurement uncertainty will increase as FN decreases. Physical limits on the manufacturable sizes of lenses and mirrors and on

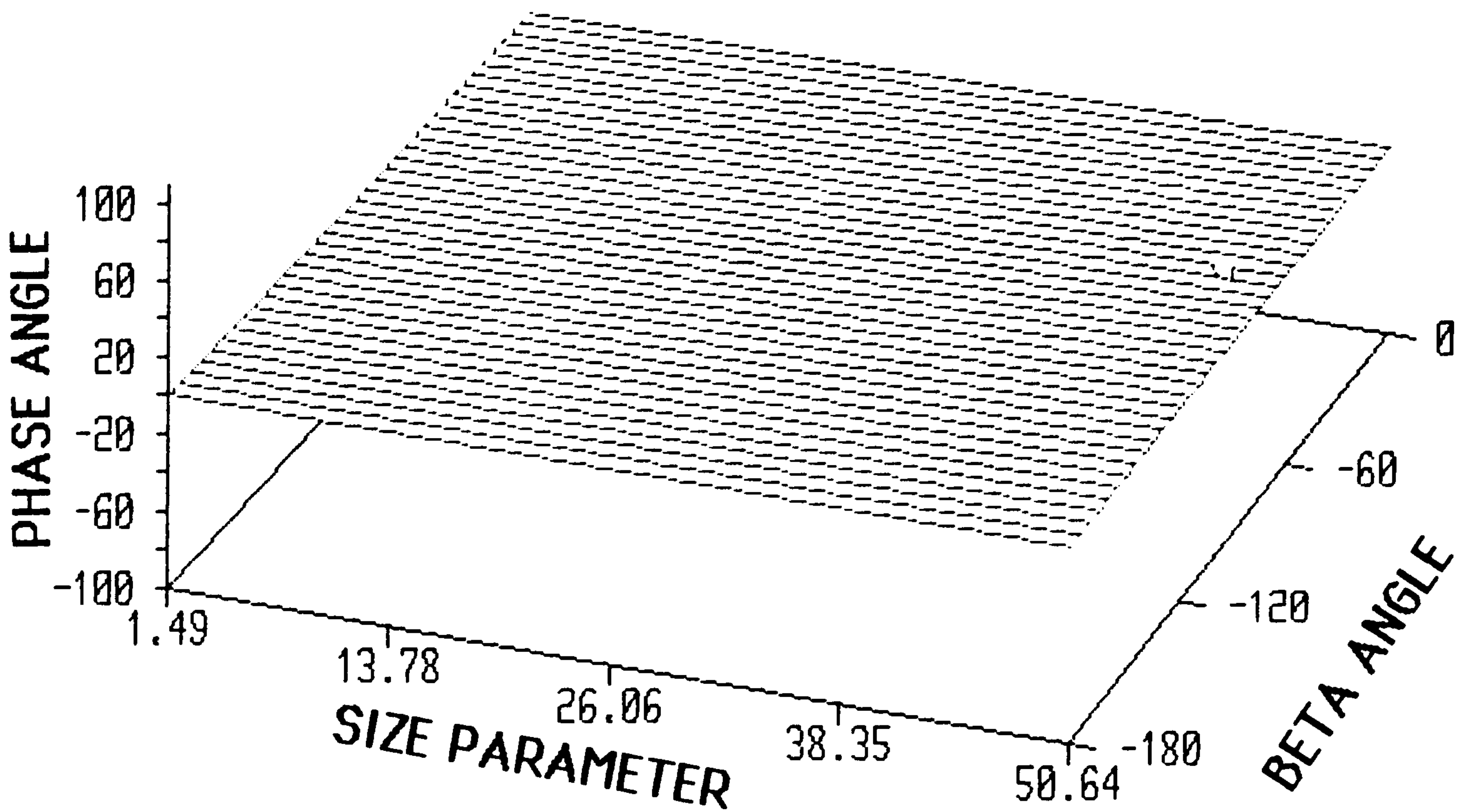

Figure 17. α Effects: $\alpha = 0°$, $\beta = 0° - 180°$, FN = 1, $\delta = 5\ \mu m$, $m = 1.7$, $\vec{E}_x$.

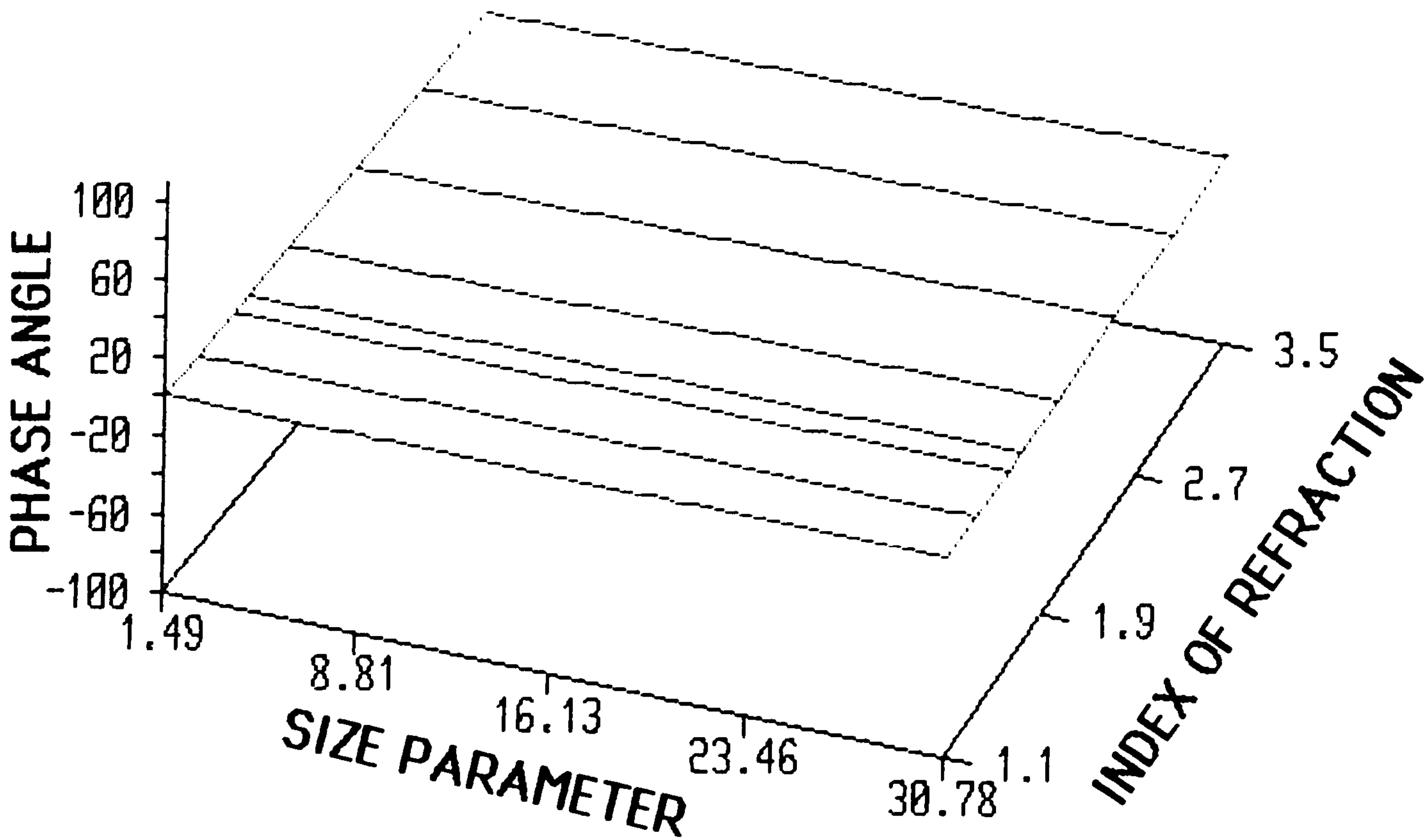

Figure 18. α Effects: $\alpha = 0°$, $\beta = 45°$, FN = 1, $\delta = 5\ \mu m$, $m = 1.1, 1.334, 1.592, 1.7, 2.0, 2.5, 3.0, 3.5$, $\vec{E}_x$.

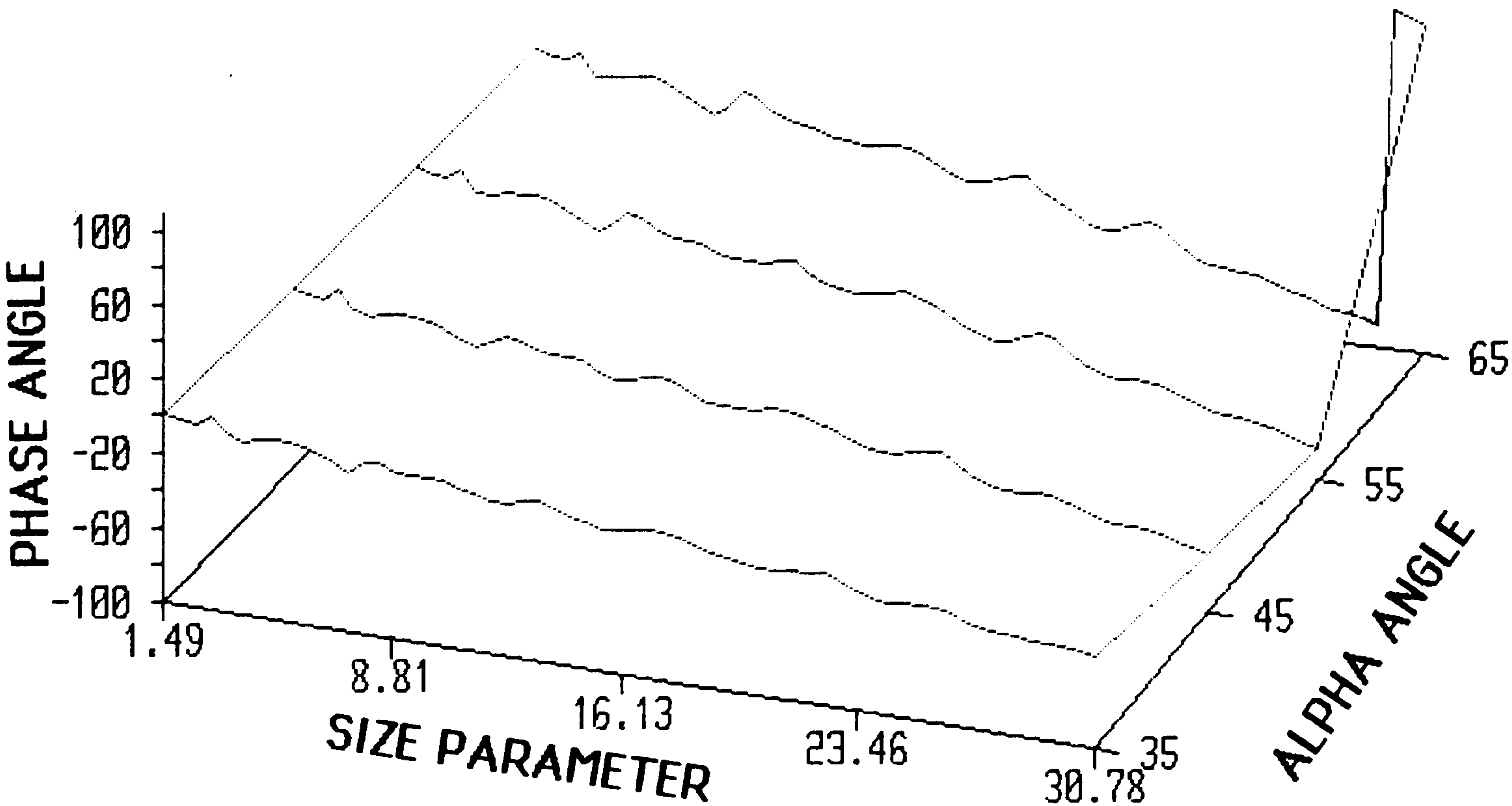

Figure 19. α Effects: $\beta = 55°$, $\alpha = 35°, 45°, 55°, 65°$, FN = 1, $\delta = 5\ \mu m$, $m = 2.5$, $\vec{E}_x$.

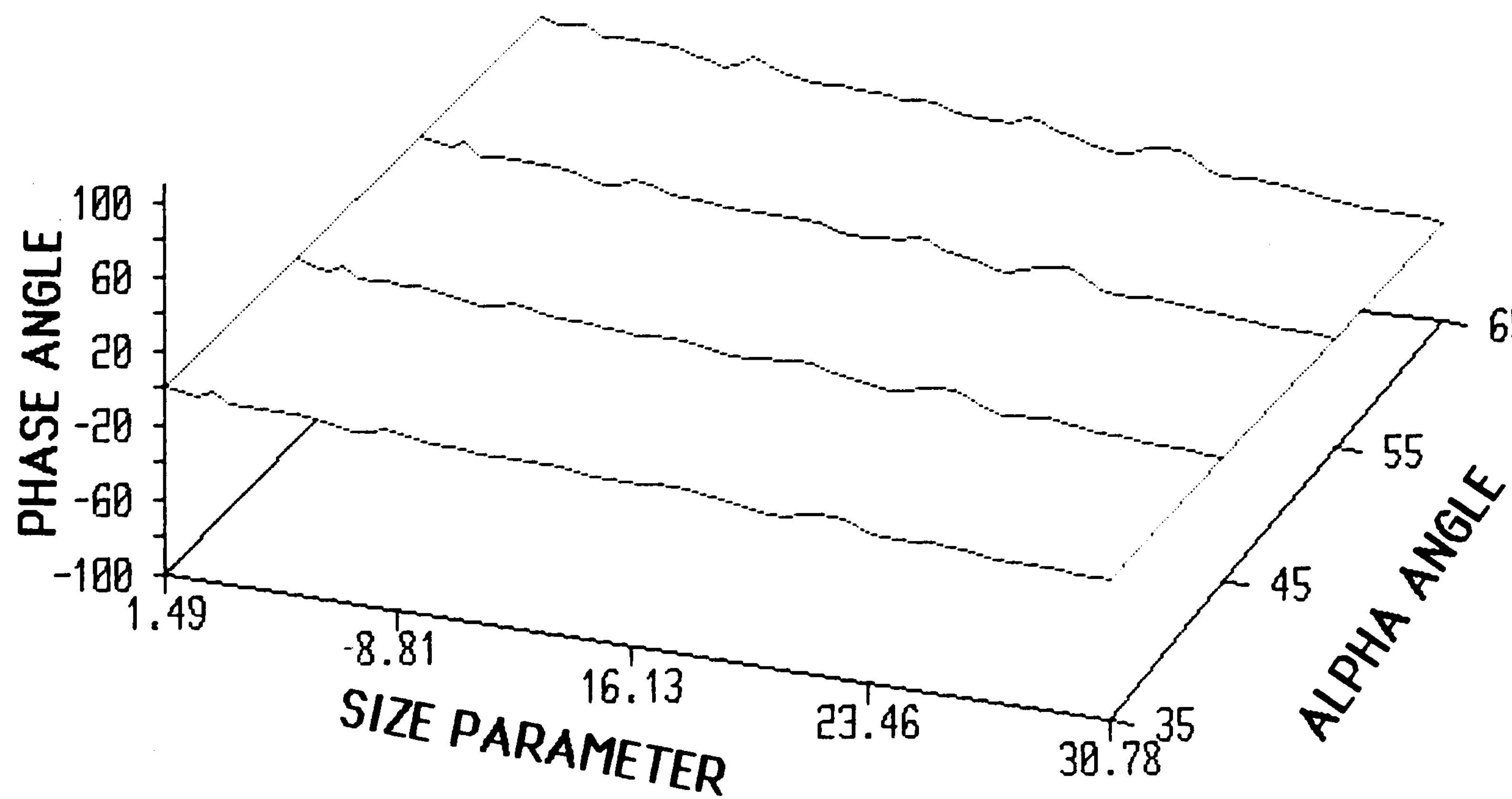

Figure 20. α Effects: $\beta = 70°$, $\alpha = 35°, 45°, 55°, 65°$, FN = 1, $\delta = 5\ \mu m$, $m = 2.5$, $\vec{E}_x$.

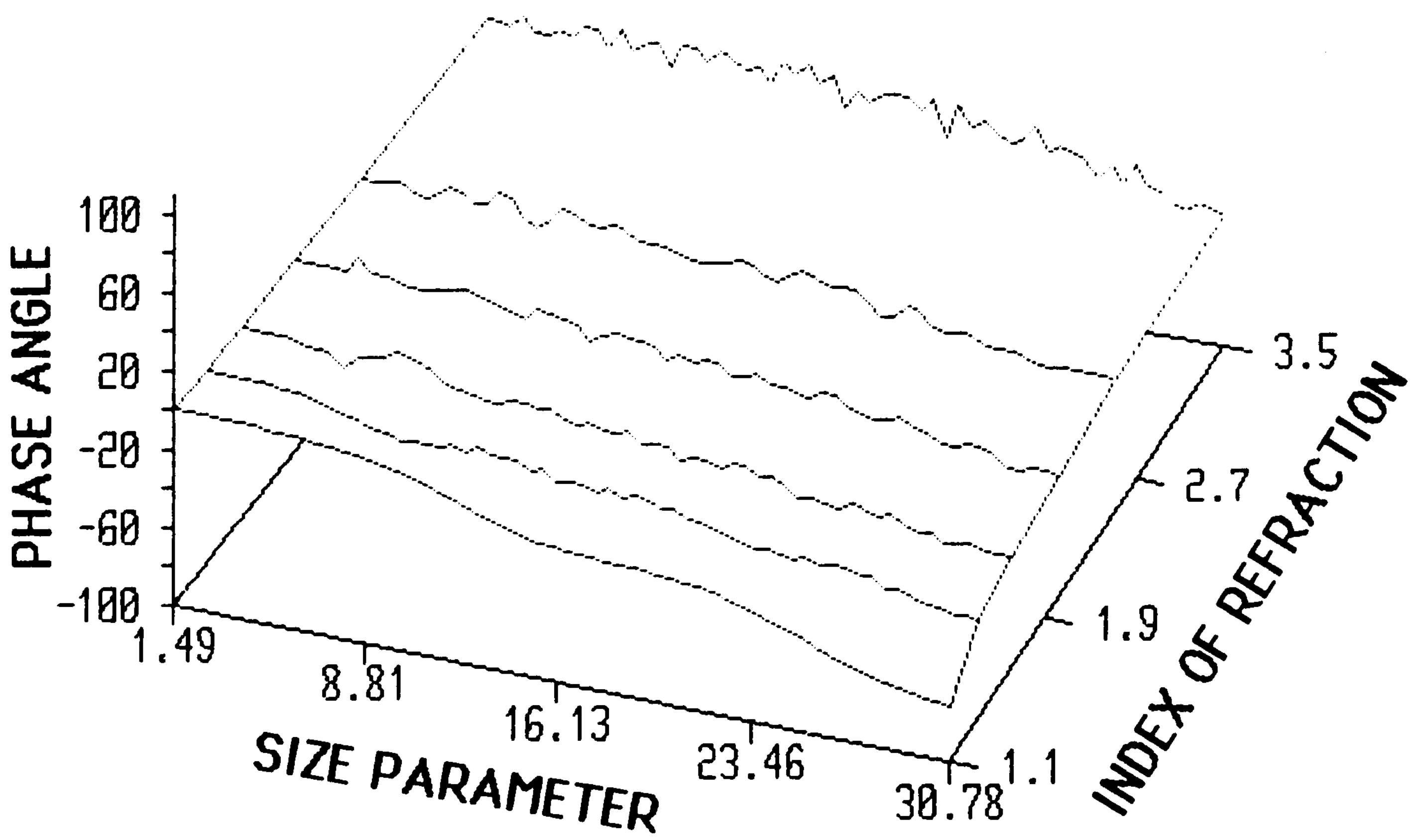

Figure 21. Index of Refraction Effects: $\alpha = 15°$, $\beta = 35°$, FN = 1, $\delta = 5$ μm, m = 1.1, 1.334, 1.592, 2.0, 2.5, 3.5, $\vec{E}_x$.

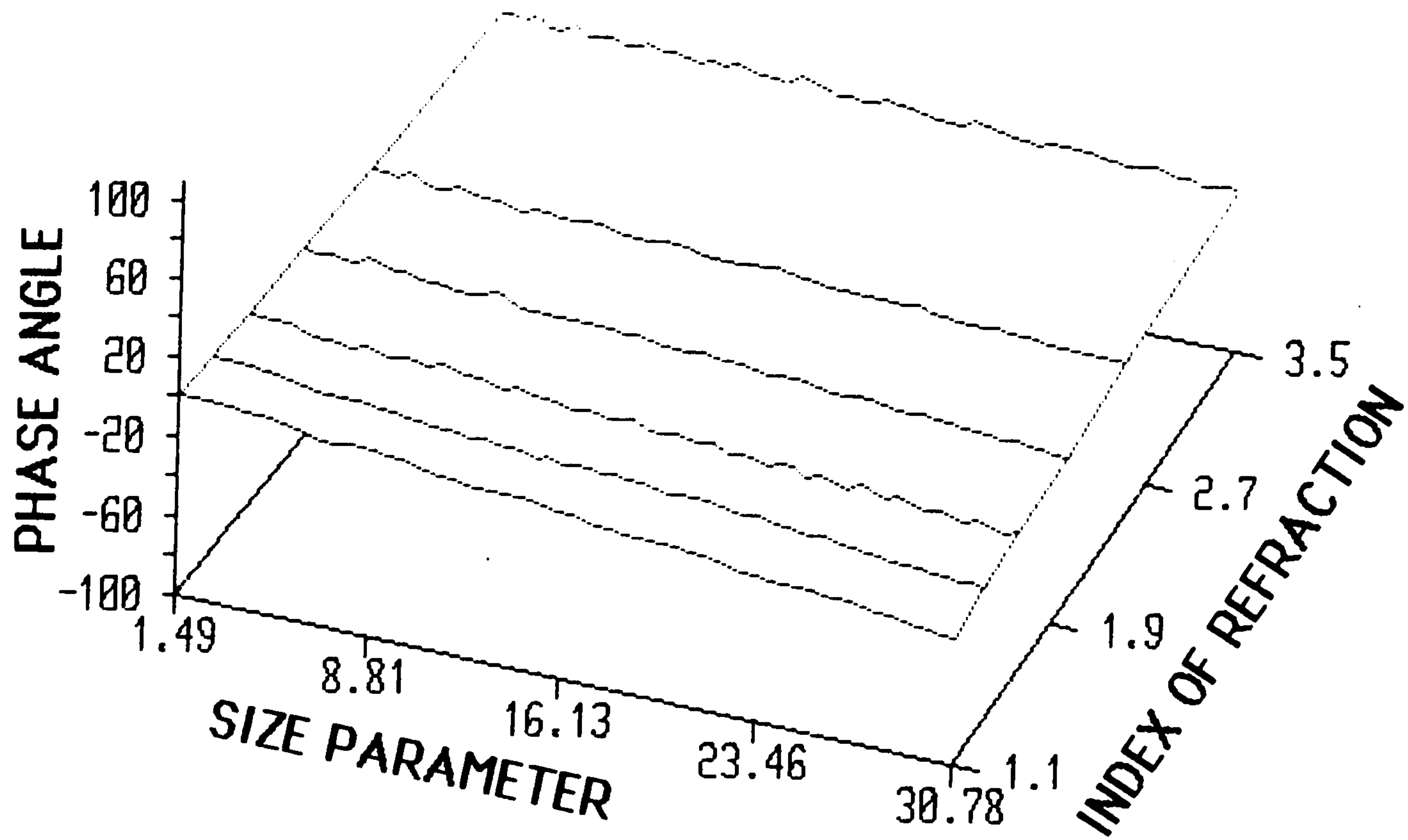

Figure 22. Index of Refraction Effects: $\alpha = 15°$, $\beta = 55°$, FN = 1, $\delta = 5\ \mu m$, m = 1.1, 1.334, 1.592, 2.0, 2.5, 3.5, $\vec{E}_x$.

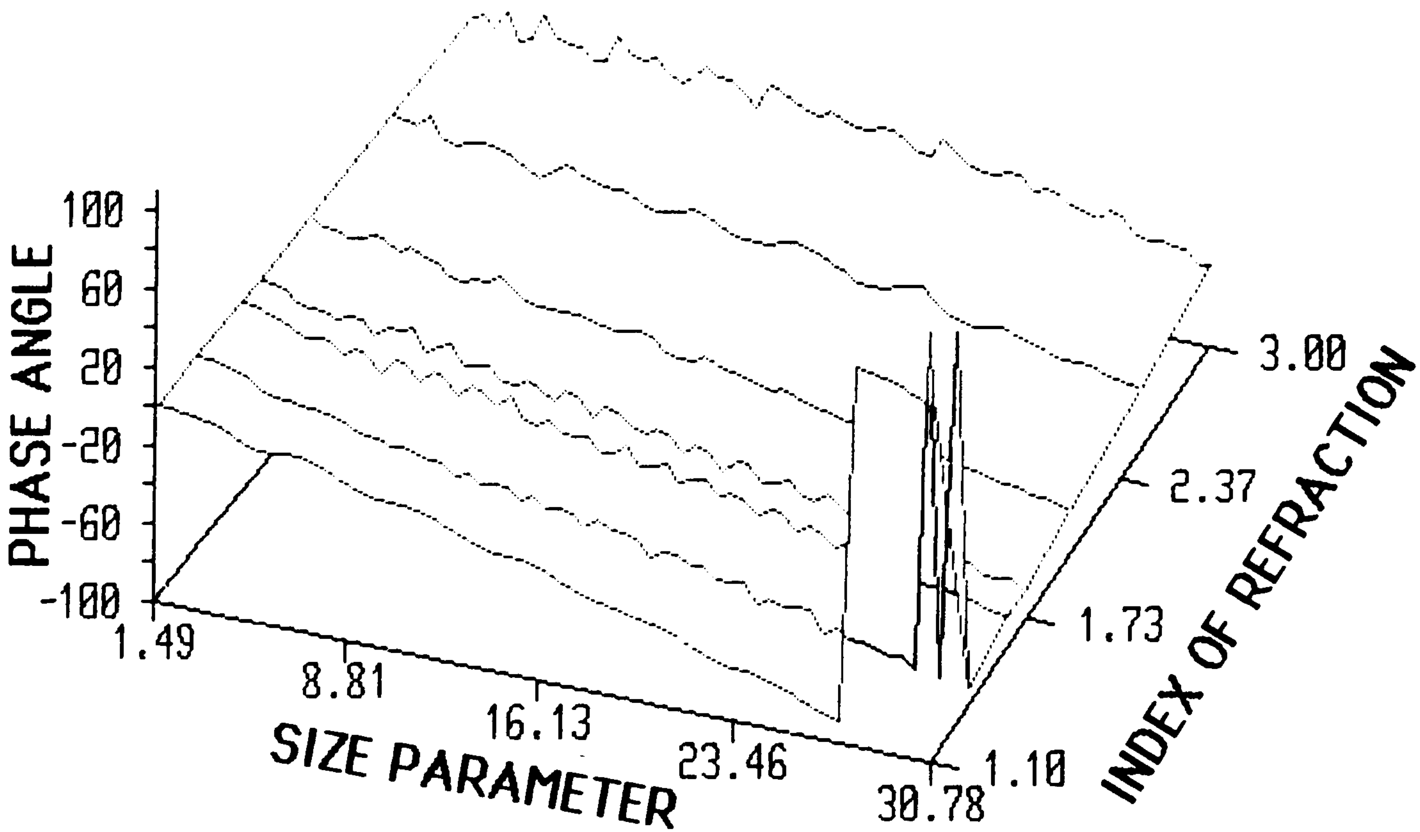

Figure 23. Index of Refraction Effects: $\alpha = 45°$, $\beta = 55°$, FN = 1, $\delta = 5\ \mu m$, m = 1.1, 1.334, 1.592, 1.7, 2.0, 2.5, 3.0, $\vec{E}_x$.

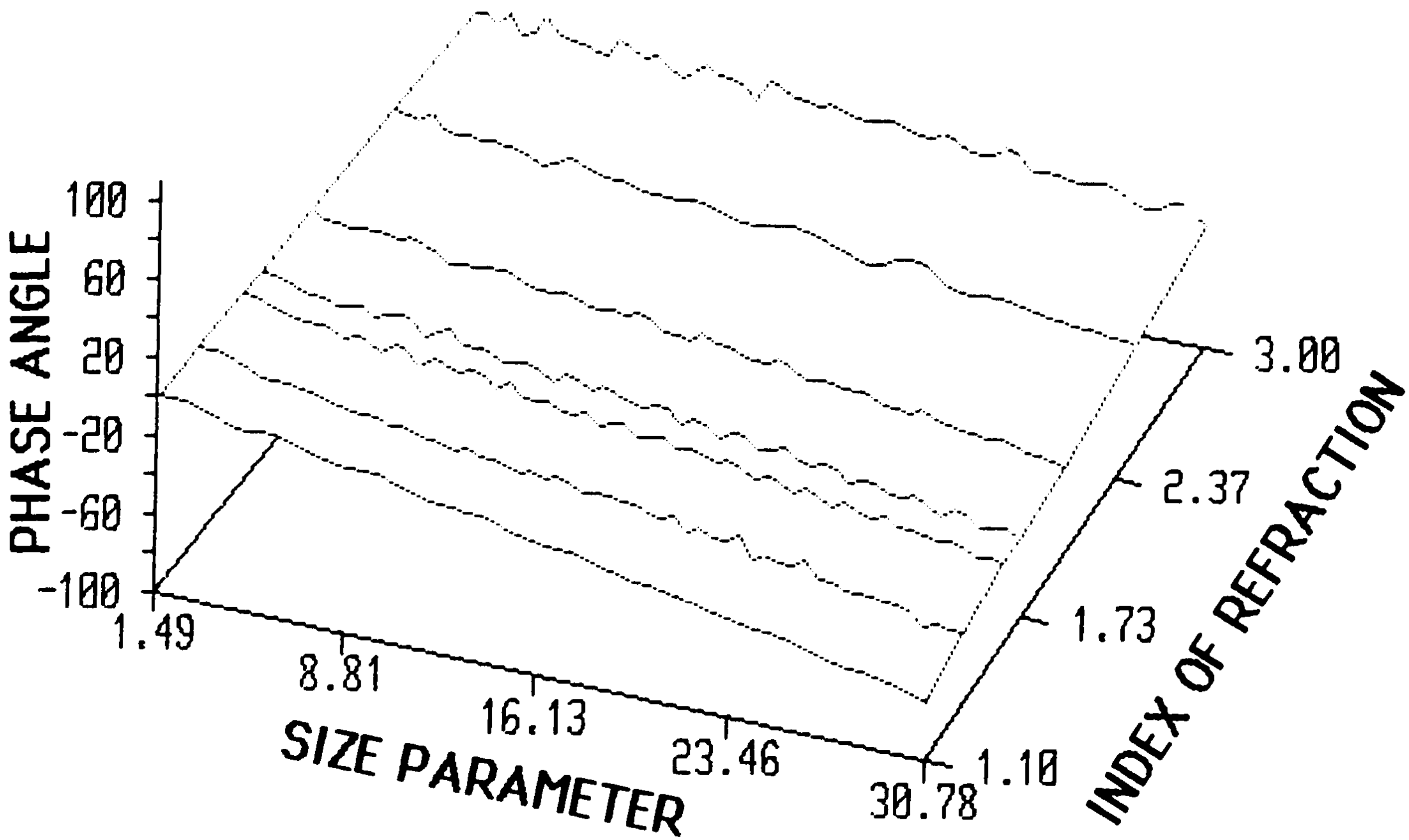

Figure 24. Index of Refraction Effects: $\alpha = 45°$, $\beta = 65°$, FN = 1, $\delta = 5\ \mu m$, m = 1.1, 1.334, 1.592, 1.7, 2.0, 2.5, 3.0, $\vec{E}_x$.

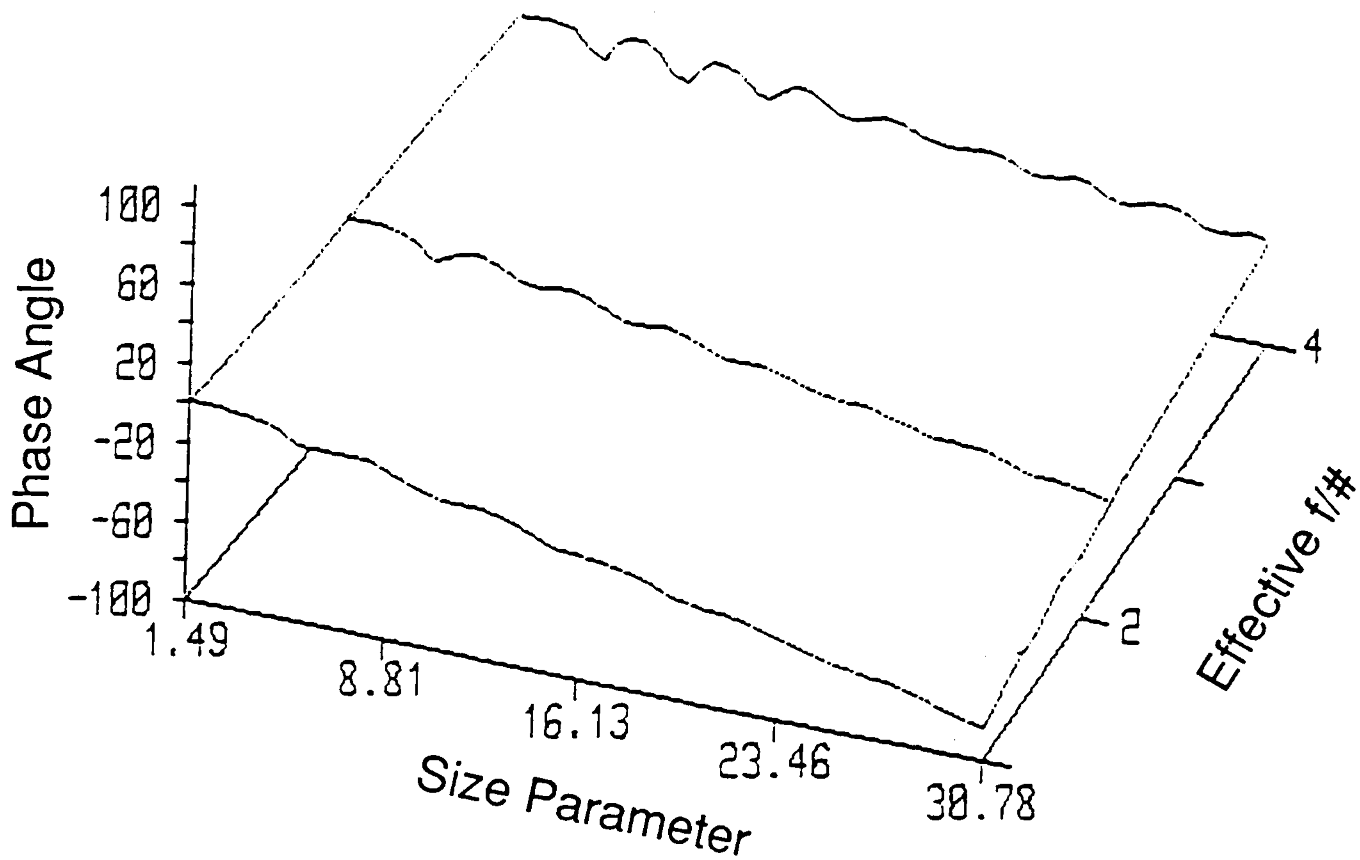

Figure 25. FN Effects: $\alpha = 35°$, $\beta = 55°$, $\delta = 5\ \mu m$, $m = 1.1$, $\vec{E}_x$.

optical access ports will limit the minimum collector FN value in a given application, but the smallest FN value attainable should be employed for phase particle sizing. The phase-size curves become smoother, as FN decreases, or equivalently as collector diameter increases for the given index of refraction. These variations are shown for $\alpha = 35°$, $\beta = 60°$, $\delta = 5\ \mu m$, $\lambda = 6328$ Angstroms, and $\vec{E}_x$ polarization.

Calculations for different polarizations are shown in Figures 26 through 29. In Figures 26 and 28, $\vec{E}$ is parallel to the x-axis ($\vec{E}_x$ polarization) and in Figures 27 and 29, $\vec{H}$ is parallel to the x-axis ($\vec{H}_x$ polarization). Figures 26 and 27 show the phase size curves for β variation with $\alpha = 45°$, FN = 1, $\delta = 5\ \mu m$, and m = 1.334. Figures 28 and 29 show the phase-size curves for index of refraction variations with $\alpha = 15°$, $\beta = 45°$, FN = 1, and $\delta = 5\ \mu m$. There is very little difference between Figures 26 and 27 and also between Figures 28 and 29, indicating that polarization has little effect. The only observable difference is in the magnitude of the smoothness of the phase size curves. The $\vec{E}_x$ curves are smoother, with a smaller magnitude in the non-monotonic variations, than the $\vec{H}_x$ curves.

The fringe period effects are shown in Figure 30 for $\alpha = 15°$, $\beta = 45°$, FN = 1, and m = 1.334. As the fringe period increases, the sensitivity decreases. The same phase change range corresponds to size range that increases nearly linear with fringe period [10]. Although the sensitivity decreases, the phase-size curves become smoother with increasing fringe spacing. In addition, the size parameter value corresponding to the first sudden jump in phase increases

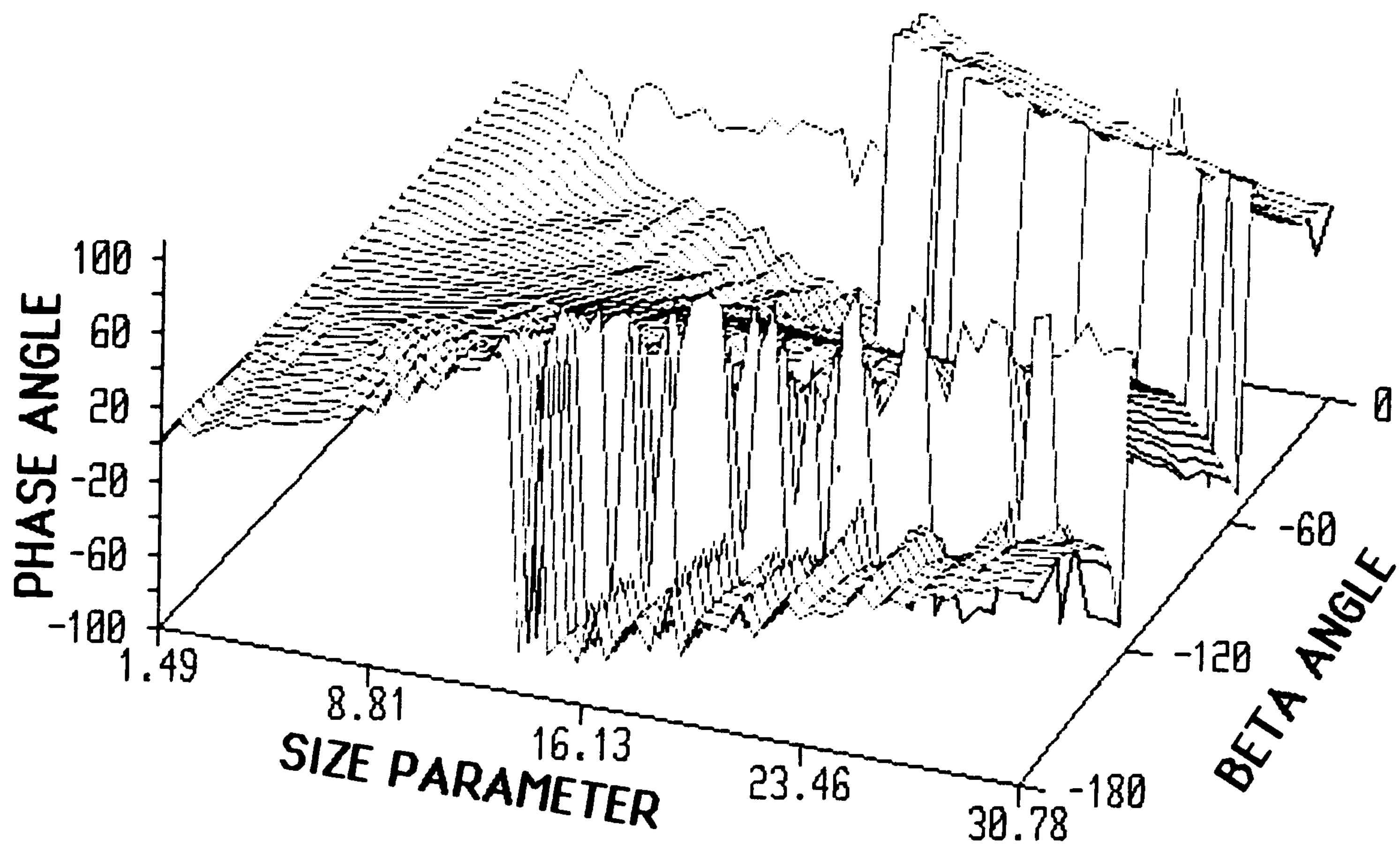

Figure 26. Effects of Polarization: $\alpha = 45°$, FN = 1, $\delta = 5$ μm, $m = 1.334$, $\beta = 0° - 180°$, $\vec{E}_x$.

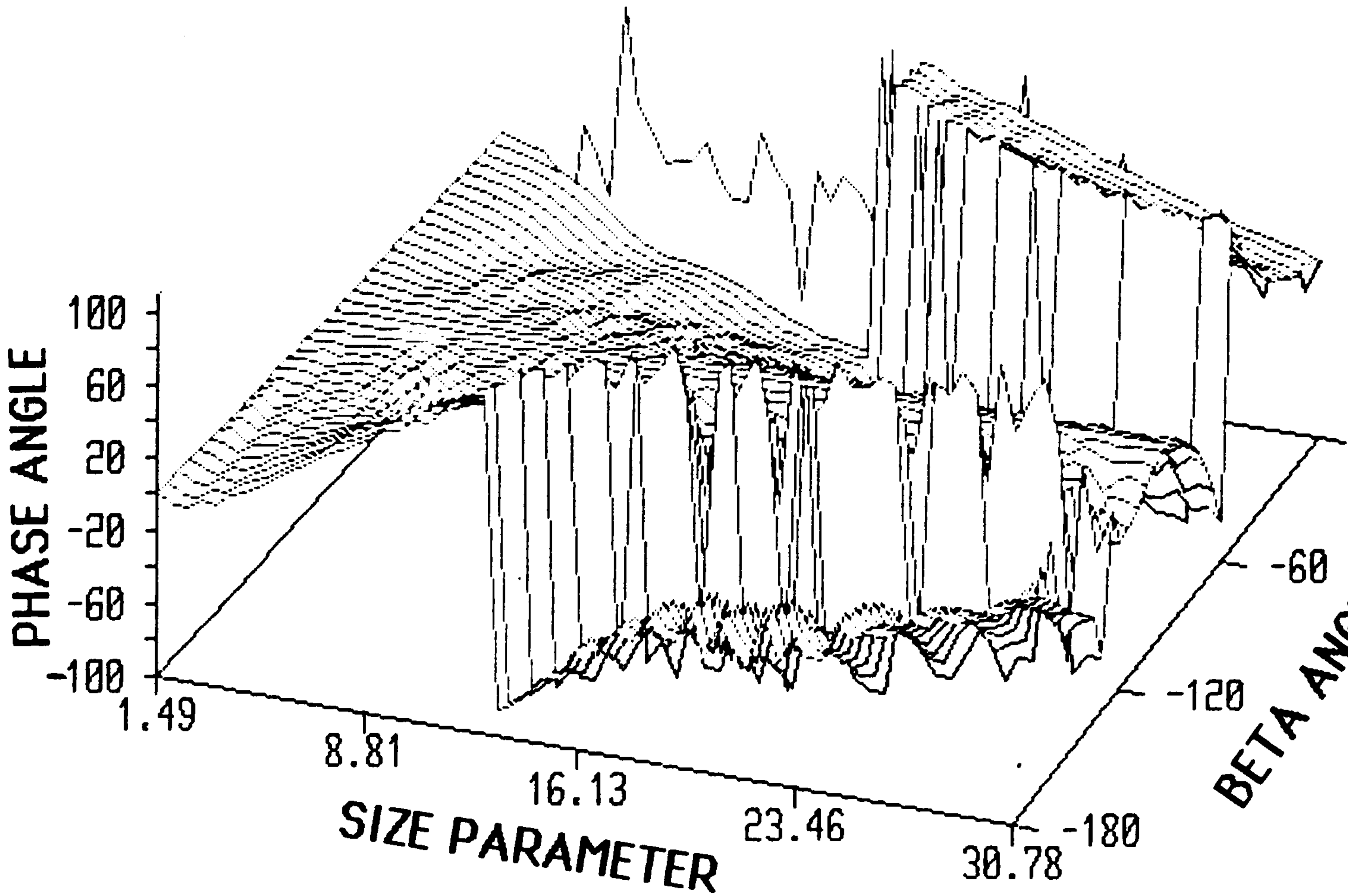

Figure 27. Effects of Polarization: $\alpha = 45°$, FN = 1, $\delta = 5$ μm, $m = 1.334$, $\beta = 0° - 180°$, $\vec{H}_x$.

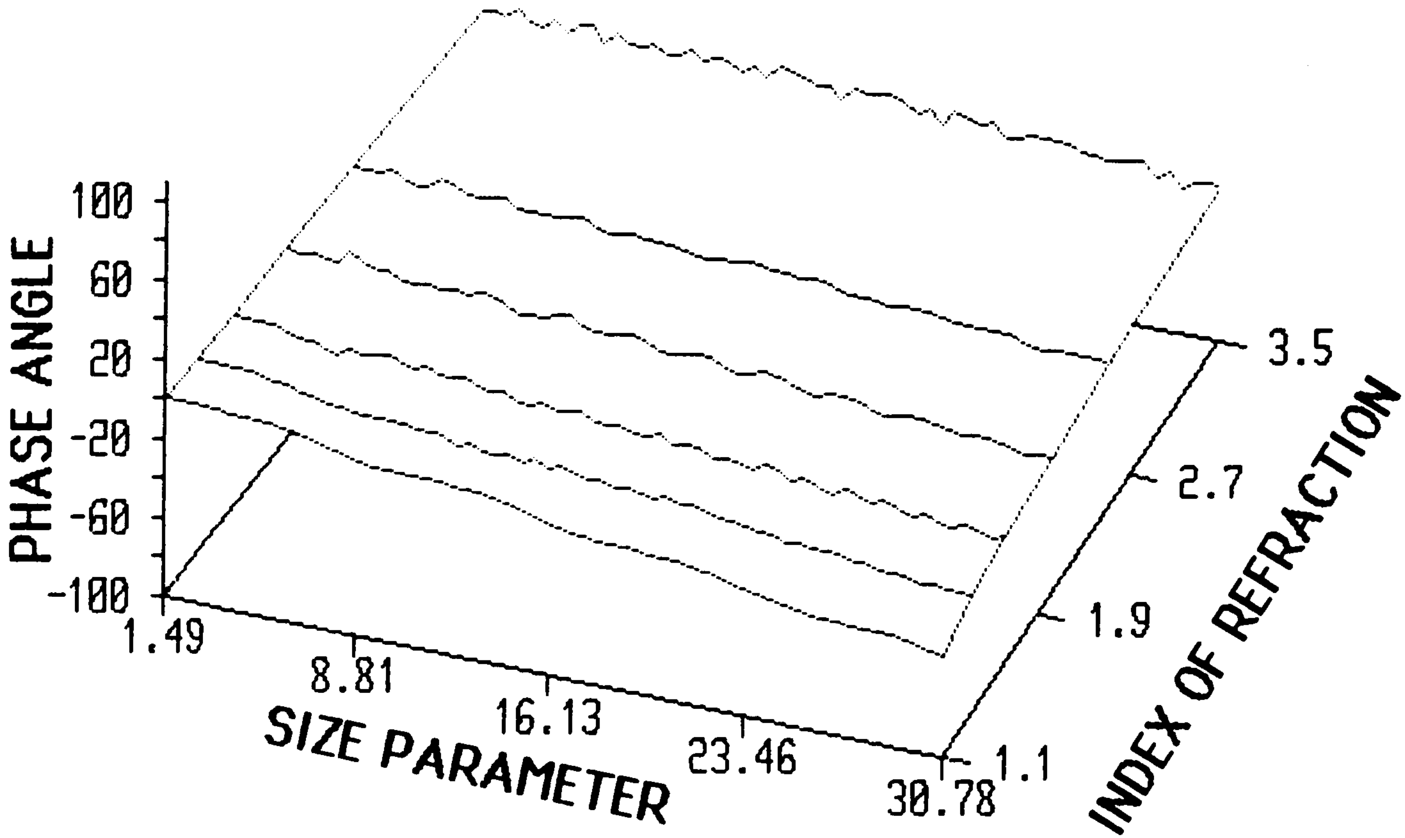

Figure 28. Effects of Polarization: $\beta = 45°$, $\alpha = 15°$, FN = 1, $\delta = 5$ µm, m = 1.1, 1.334, 1.592, 2.0, 2.5, 3.5, $\vec{E}_x$.

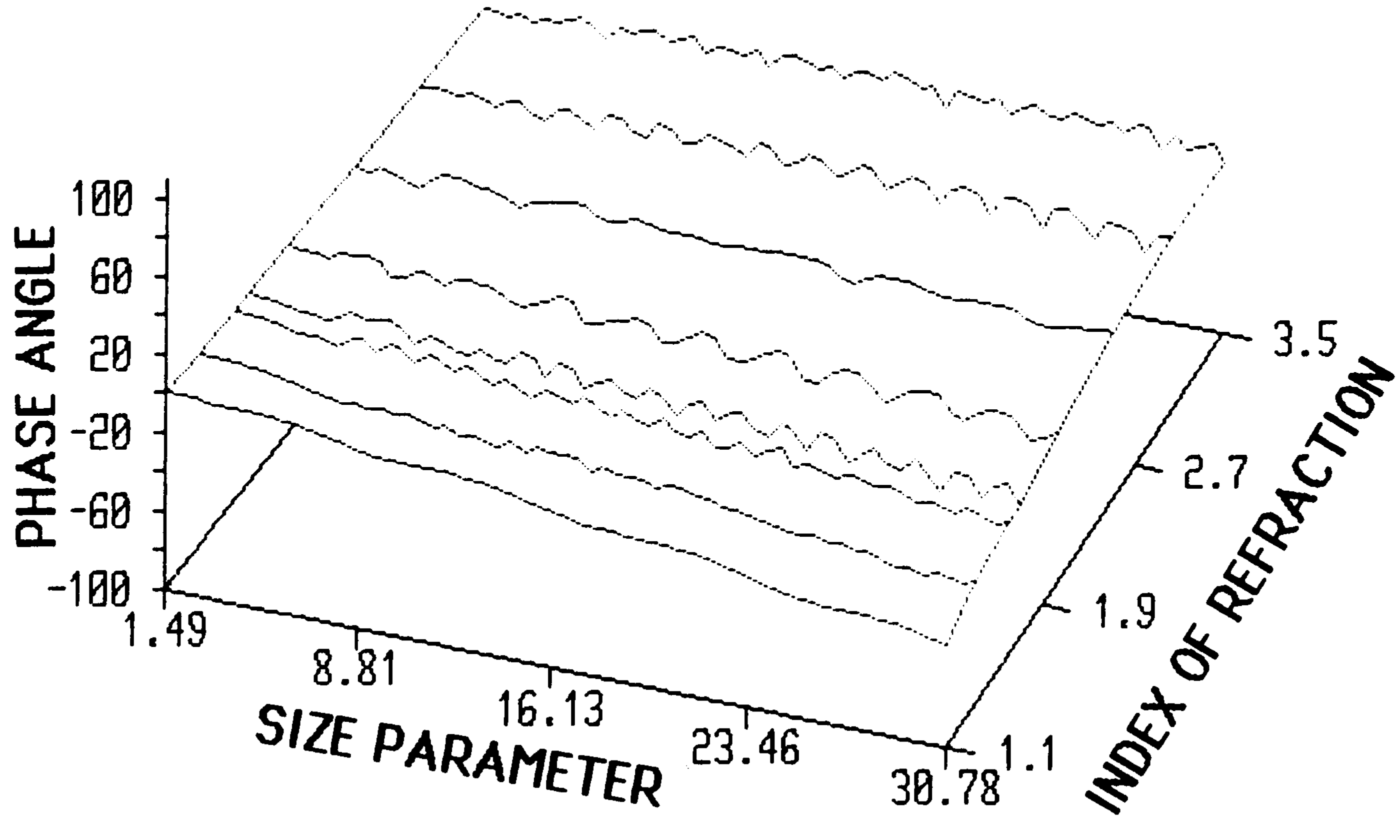

Figure 29. Effects of Polarization: $\beta = 45°$, $\alpha = 15°$, FN = 1, $\delta = 5\ \mu m$, $\underline{m}$ = 1.1, 1.334, 1.592, 1.7, 2.0, 2.5, 3.0, 3.5, $\vec{H}_x$.

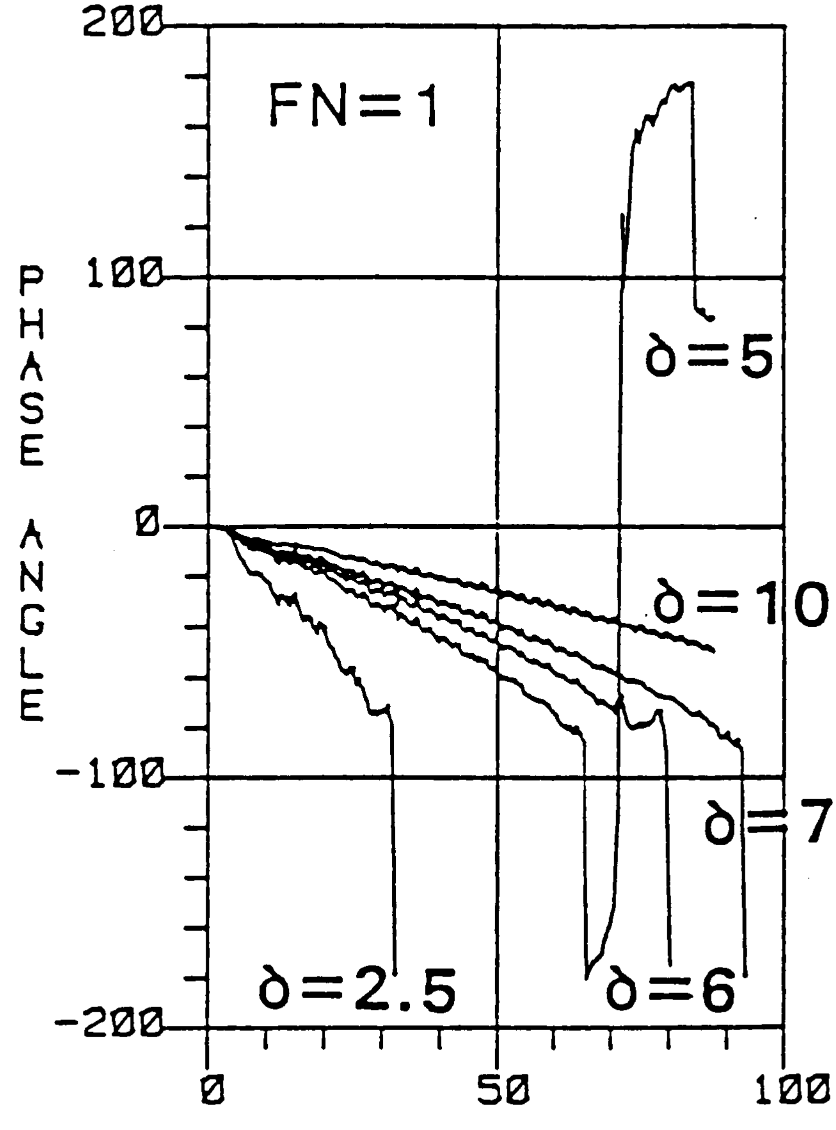

Figure 30. Effects of Fringe Period: $\alpha = 15°$, $\beta = 45°$, FN = 1, $m = 1.334$, $\delta = 2.5, 5, 6, 7, 10\ \mu m$.

with increasing fringe spacing, resulting in a larger usable particle sizing range. Finally, for all fringe periods, the approximate particle size showing a 0° phase shift occurs for a size parameter of 1.49. For λ = 6328 Angstroms $X = 1.49$ corresponds to a particle size of 0.3 μm. Thus the minimum particle size which can be measured using phase and a Helium-Neon laser is 0.3 μm, even for a fringe period of only 2.5 μm. If the Argon-ion 4880 Angstrom line is used, the minimum measurable particle size decreases to 0.23 μm.

CHAPTER IV

CONCLUSIONS AND RECOMMENDATIONS

A number of collected light scattering characteristics of a dual beam laser Doppler velocimeter have been proposed as particle size indicators. The Doppler signal phase is one of the most promising indicators for particle size measurements. Phase is independent of particle trajectory, is insensitive to system gain and source intensity drifts, and has a measurable particle size range which is a function of fringe period. Phase, however is dependant on the collector lens location, given as angles α and β, and collector lens size given as 1/FN. Therefore, an optical geometry needs to be found having sufficient range, sensitivity and a sufficiently monotonic relationship between phase and particle size for each given application. The geometry selected depends on the particle size range to be encountered. Phase is also sensitive to particle index of refraction. Thus the geometry selected depends on the particle index of refraction to be encountered.

Because the range and sensitivity of phase depends so strongly on the PSI optical system geometry and particle index of refraction, results of Mie calculations need to be examined before configuring the PSI for each application. Mie calculations performed for some general optical system geometries provide the following general guidelines for selection of optical geometries.

1. Increasing β, locating the collector aperture, increases the measurable size parameter range, and decreases the number

and amplitude of non-monotonic variations in the phase-size parameter curves. However, increasing β decreases the sensitivity of phase to size parameter.

2. Decreasing α, locating the collector aperture, also increases the measurable size parameter range, improves the smoothness of the phase-size parameter curves, and decreases the sensitivity of phase to size parameter. For $\alpha = 0°$ no phase changes occur with size parameter.

3. Increases in index of refraction cause the amplitude and number of non-monotonic variations in the phase-size parameter curves to increase and the size parameter range corresponding to a given phase range to increase (i.e., a decrease in sensitivity.) Thus sizing using phase will have smaller measurement uncertainties for smaller particle index of refraction if the same optical geometry is employed. An evaluation should be performed for absorptive particles (having a non-zero imaginary index of refraction component). Extremely long computational times prevented performing this evaluation during the present investigation.

4. As collecting aperture increases (FN decreases) the smoothness of the phase-size parameter curves improves and the sensitivity also increases. Thus the largest collecting aperture possible is recommended for phase sizing.

5. Polarization has very little effect on phase, but an $\vec{E}_x$ polarization offers slight improvements over an

$\vec{H}_x$ polarization for phase sizing. More calculations should be performed to further verify this conclusion.

6. As the fringe period increases, the sensitivity of phase decreases, the usable size range increases and the smoothness of the phase-size parameter curves improves. The minimum particle size which can be measured using phase is 0.3 μm for a laser wavelength of 6328 Angstroms for the configurations considered. However, since the effect of fringe period is significant, and only a few calculations were performed for fringe period variations, more calculations need to be performed to further delineate the effects of fringe period variations, and the minimum resolvable particle size.

As shown by Saffman, et al. [13], non-spherical particles can be identified, but the theory for sizing with phase is not developed. After a full Mie evaluation is performed, using a geometry identified for spherical particle sizing, an evaluation should be performed for non-spherical particles. A different theory will have to be developed for this non-spherical particle evaluation, however, so the problem of detection and sizing of non-spherical particles should be addressed by future researchers. There is also a need for experimental verification of the phase geometry dependance. However, due to the difficulties in conducting adequate experimental studies, only a few selected experiments are suggested to verify the calculated "calibrations", or provide data to indicate appropriate modifications to the calculation procedure.

It is further suggested that the uncertainties due to changes in optical geometry be quantified so selection of the best geometry for a given application can be made on the basis of resulting size measurement uncertainty rather than smoothness and resolution of the phase-size parameter curves.

LIST OF REFERENCES

LIST OF REFERENCES

1. Allen, T., Particle Size Measurement, Chapman and Hall, London, 1975.

2. Self, S. A., "Optical Diagnostic Techniques for Particulates," Advanced Diagnostics for Particle-Laden Combustion Flows, Sandia National Laboratories, Livermore, California, March 1984.

3. Hodkinson, J. R., and I. Greenleaves, "Computations of Light-Scattering and Extinction by Spheres and some Comparisons with the Mie Theory," Journal of Optical Society of America, Vol. 53, p. 577, 1963.

4. Holve, D. J., "In Situ Optical Particle Sizing Technique," Journal of Energy, Vol. 4, p. 176, 1980.

5. Holve, D. J., "Optical Size Distribution Measuring Techniques for Particles Larger than 0.1 Micrometer," Advanced Diagnostics for Particle Laden Combustion Flows, Sandia National Laboratories, Livermore, California, March 1984.

6. Son, J. Y., "Multiple Methods for Obtaining Particle Size Distribution with a Particle Sizing Interferometer," Ph.D. Dissertation, The University of Tennessee, Knoxville, Tennessee, June 1985.

7. Yeh, Y. and H. Z. Cummins, "Localized Fluid Flow Measurements with an He-Ne Laser Spectrometer," Applied Physics Letters, Vol. 4, p. 176, May 1964.

8. Farmer, W. M., "Measurement of Particle Size, Number Density and Velocity Using a Laser Interferometer," Applied Optics, Vol. 11, p. 2603, 1972.

9. Pendleton, J. D., "A Generalized Mie Theory Solution and Its Appliation to Particle Sizing Inerferometry," Ph.D Dissertation, The University of Tennessee, Knoxville, Tennessee, June 1982.

10. Son, J. Y., T. V. Giel, Jr., and V. S. Waddell, "Analysis of Scattering Characteristics of Particle Sizing Interferometer," Proceedings of The Third International Symposium on Applications of Laser Anemometry to Fluid Mechanics, Lisbon, Portugal, 1986.

11. Durst, F., and M. Zare, "Laser Doppler Mesurements in Two Phase Flows," SFB80/TM/63, University Karlsruhe.

12. Bachalo, W. D., and M. J. Houser, "Spray Analyzer for Simultaneous Measurements of Drop Size and Velocity Distributions," Optical Engineering, 23, 583.

13. Saffman, M., P. Buchhave and H. Tanger, "Simultaneous Measurement of Size, Concentration and Velocity of Spherical Particles by a Laser Doppler Method," Proceedings of the Second International Symposium on Appliaitons of Laser Anemometry to Fluid Mechanics, Lisbon, Portugal, 1984.

14. Chu, W. P. and D. M. Robinson, "Scattering From a Moving Spherical Particle by Two Crossed Coherent Plane Waves," Applied Optics, Vol. 16, p. 619, 1977.

15. Farmer, W. M., Optical Methods of Aerosol Characterization, The University of Tennessee Space Institute, Tullahoma, Tennessee.

16. Pendleton, J. D., "Mie Scattering Theory for Particle Sizing Interferometry with the Dual Beam Laser Velocimeter," DOE Topical Report under Contract No. DE-AC02-79ET10815, February 1983.

17. Mie, G., Annalen der Physik, Band 25, p. 377, 1908.

18. Dave, J. V., "Subroutines for Computing the Parameters of the Electromagnetic Radiation Scattered by a Sphere," IBM Palo Alto Scientific Center Report N320-3237, May 1968.

19. Wiscomb, W. J., "Mie Scattering Calculations: Advances in Technique and Fast, Vecator-Speed Computer Codes," NCAR/TN-140 + STR, June 1979.

20. Cylek, P., "Mie Scattering into the Backward Hemisphere," Journal of the Optical Society of America, Vol. 63, p. 1467, 1973.

21. Pendleton, J. D., "Mie Scattering into Solid Angles," Journal of the Optical Society of America, 72, p. 1029, 1982.

22. Rose, M. E., Elementary Theory of Angular Momentum, John Wiley, New York, 1957.

23. Son, J. Y., and T. V. Giel, Jr., "Mie Scattering Program for Evaluating Radiatn Power Scattered into a Cone Centered at any Direction," DOE Internal Report No. OR-10815-13, December 1984.

24. The University of Tennessee Space Institute Energy Conversion Research and Development Programs, "In-Situ Particle Characterization," Quarterly Technical Progress Report, February 1986.

25. Lentz, W. J., "Generating Bessel Functions in Mie Scattering Calculations Using Continued Functions," Applied Optics, Vol. 15, p. 668, 1976.

APPENDIX

evaluated is given by:

Particle size range = (DODBA) to (DODBA + NOSETS DODEL)

3. ALAMD, DELTA, FNO, KCRITE

ALAMD: Wavelength of the light to be used, given in microns.

DELTA: Fringe period of the two crossed laser beams, δ, given by $\delta = \lambda/2\sin(\theta)$

θ is half the incidence angle of the two crossed light beams (Note that n, the fluid index of refraction, is taken as 1.0)

FNO: The effective f-number of the collecting lens $\#f_e$, ($\#f_e$ = distance from the probe volume to the center of the receiving lens/ receiving lens diameter.)

KCRITE: Constants for choosing the proper minimum value of $|\text{Term}|$. In this program, KCRITE can have values 1 to 10, corresponding to minimum values of Term of 10^{-6} to 10^{-18}.

4. ALPHZ, BETAZ, ANGIN, STBETA, JCRITE

ALPHZ and BETAZ represent the position of the collecting lens in Cartesian coordinates. Their values are given in degrees.

ALPHZ: The angle of rotation about the x-axis. (1 to 180°) (See α, Figure 3)

BETAZ: The angle of rotation about the y'-axis. (0 to 180°) (see β, Figure 3)

ANGIN: The inner radius of the receiving lens, given in degrees. (This inner radius defines beam stop size.)

STBETA: Starting value of the BETAZ angle. From this angle the scattered intensity distribution can be evaluated ITNUM times with the angle increment specified by DEGINC.

JCRITE: This represents whether the receiving aperture location is symmetric with respect to the beams

1 represents a symmetrical loation

2 represents an asymetrical loation

5. ITNUM, DEGINC, JAF, MPOLA, ADDANG, POLANG

ITNUM: The set of data given by NOSET will be calculated ITNUM times with different BETAZ angles. There is no limit to ITNUM, but ITNUM x DEGINC should be $\leq 180°$.

DEGINC: Specifies the increment of BETAZ angles

JAF: The same representation as JCRITE but JAF = 3 represents the symmetric case and JAF = 4 represents the asymmetric case.

MPOLA: Specifies the laser beams polarization direction. When MPOLA = 1, $\vec{H}$ is parallel to the x-axis. When MPOLA = 0, $\vec{E}$ is parallel to the x-axis.

ADDANG: Specifies a certain BETAZ angle to be calculated. When ADDANG is specified, DEGINC does not apply to this angle.

VITA

Voreata Anne Sanders Waddell was born on March 8, 1948 in Rogersville, Tennessee. She received a Bachelor of Arts Cum Laude in Mathematics and Latin-Greek from The University of Tennessee Chattanooga in May 1979. She received a Bachelor of Science Magna Cum Laude in Physics from The University of Tennessee Chattanooga in May 1984. During that time she was employed by the Mathematics Department at UTC as an instructor in mathematics, serving as Acting Director and later as Assistant Director of Developmental Mathematics.

In September 1984 she entered The University of Tennessee Knoxville as a Graduate Research Assistant in the Gas Dynamics Section of the Energy Conversion Research and Development Programs at The University of Tennessee Space Institute and received the Master of Science degree with a major in Physics in August 1986.

She is a member of the honor societies of Pi Mu Epsilon and Sigma Pi Sigma, a member of Tennessee Mathematics Teachers Association, Chattanooga Area Mathematics Teachers Association, and a student member of The American Society of Mechanical Engineers (ASME).